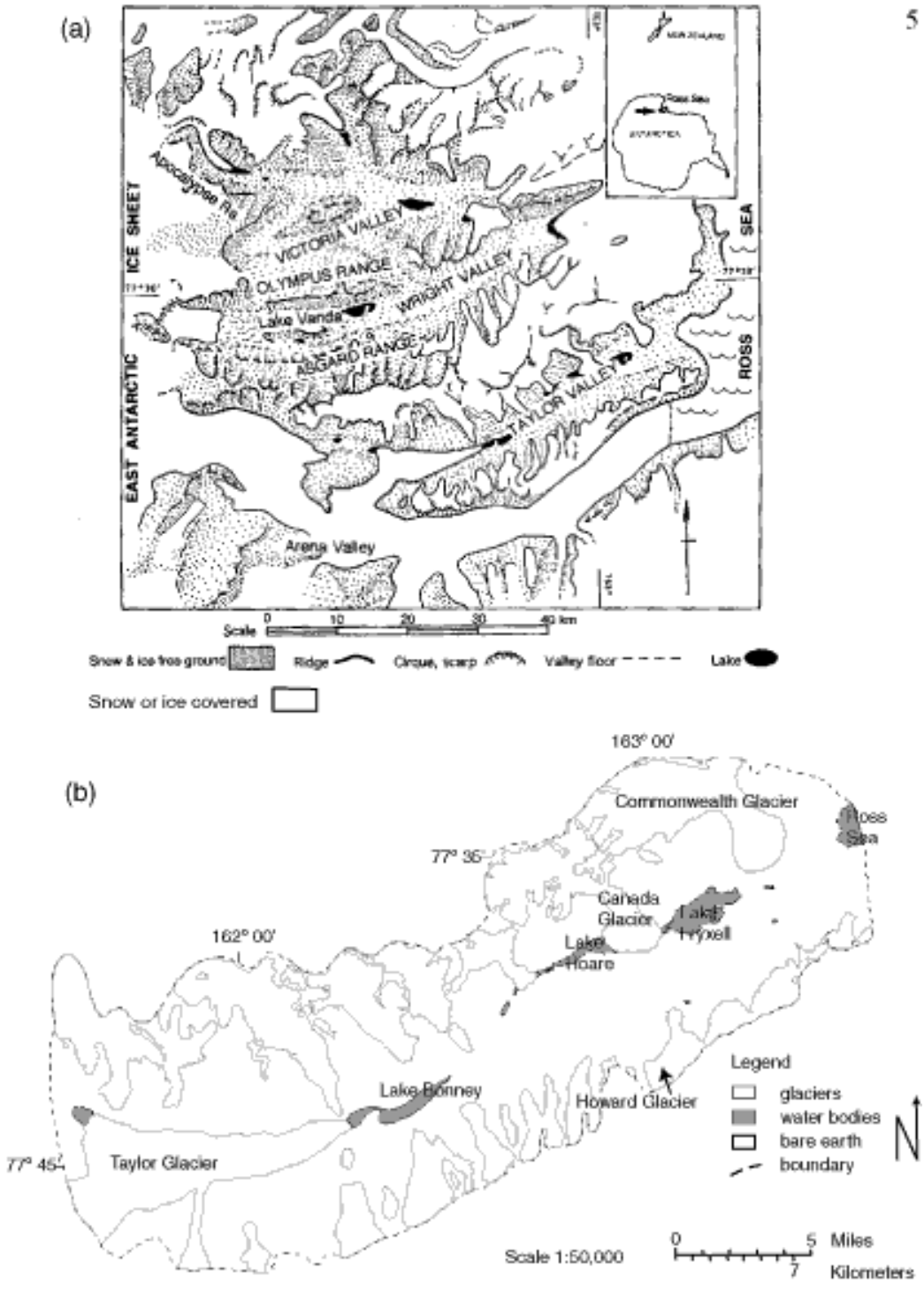

Figure 1.1: site maps. (a) The McMurdo Dry Valleys (Chinn, 1996), (b) Talor Valley (INSTAAR MCM Long-Term Ecological Research website).

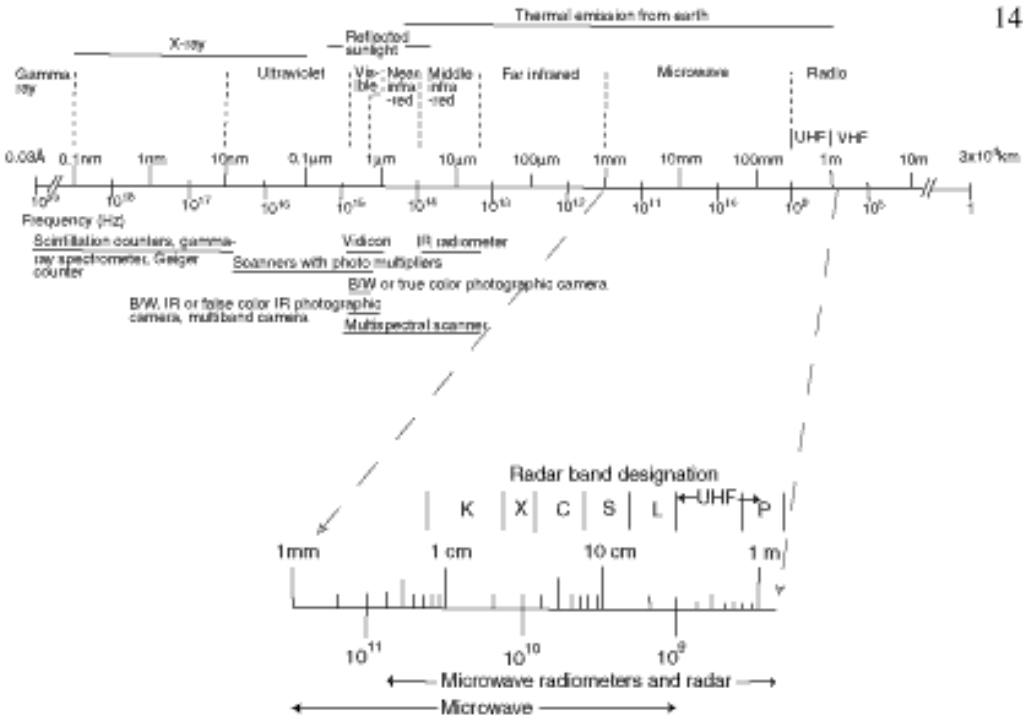

Figure 3.1: The electromagnetic spectrum (Trevett, 1986).).

17

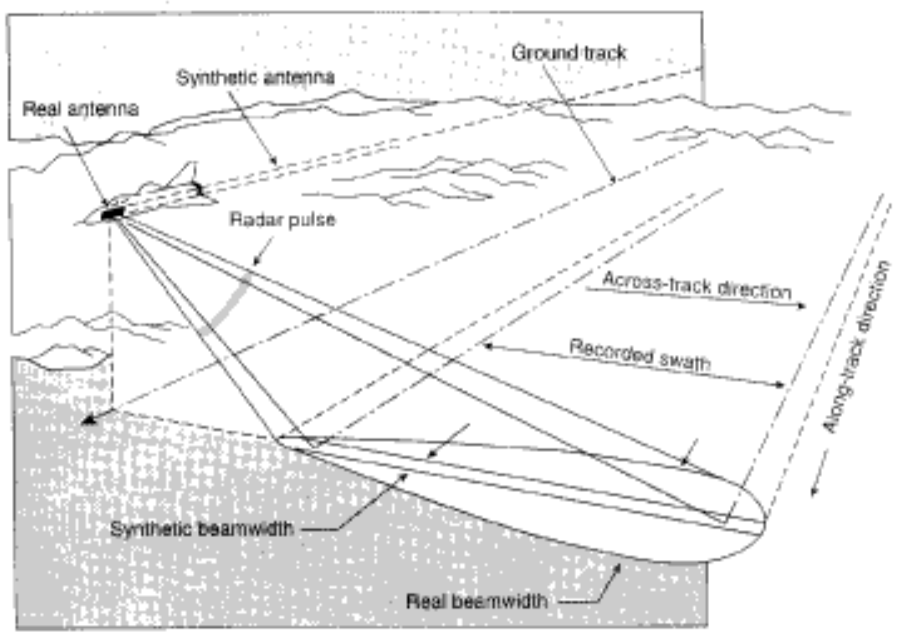

Figure 3.2: Operating principle of a SAR (Avery and Berlitir 1992).

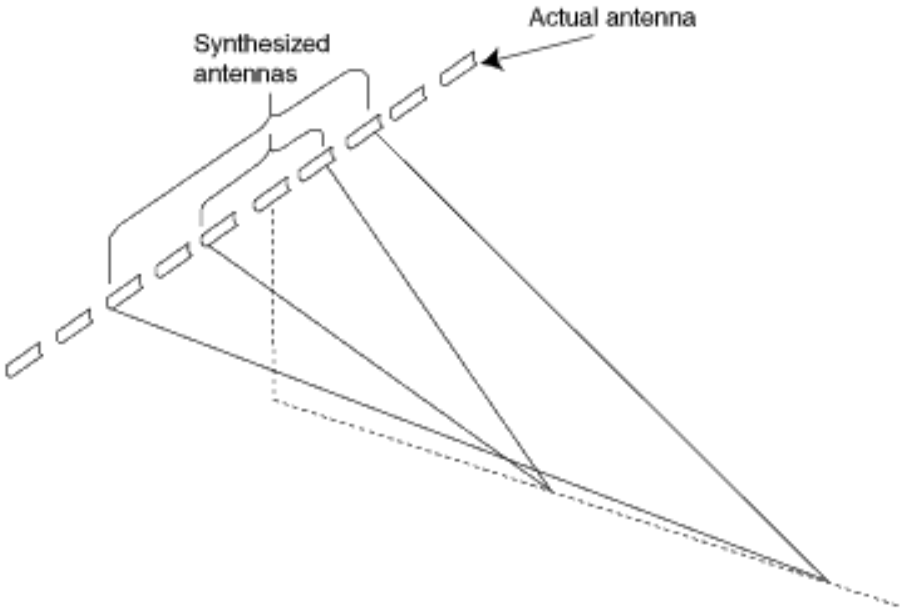

Figure 3.3: Concept of an array of reaaantenna positions ; irming a synthetic aperture (Lillesand and Kiefer, 1994). ı.

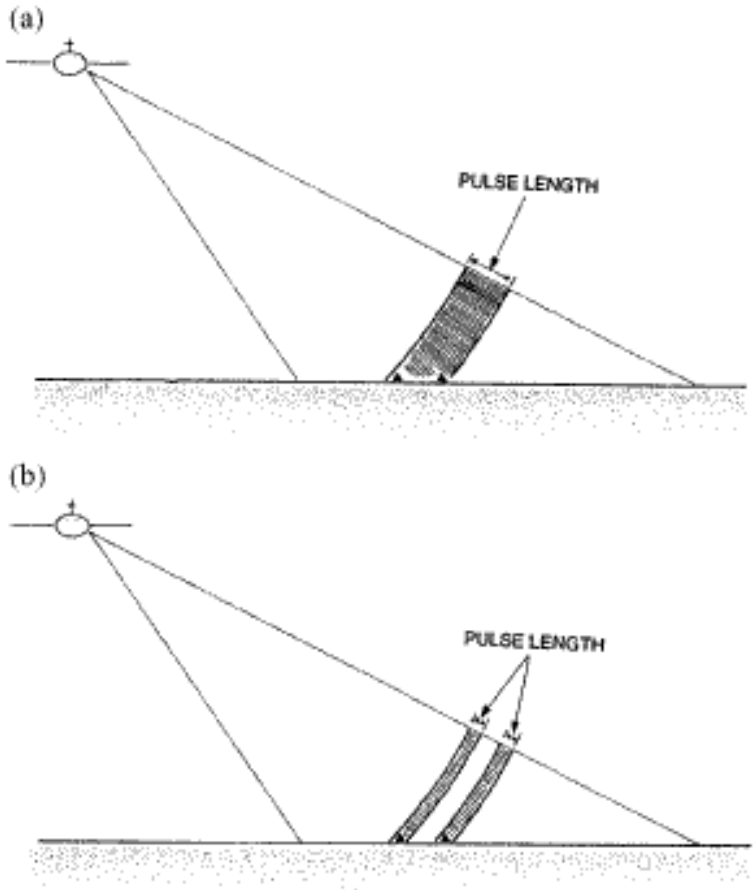

Figure 3.4: Effect of pulse length (Campbell, 1996). Long pulse length (a) causes the two objects to be illuminated by a single radar burst, creating a single return that does not resolve the two objects. Shorter pulse length (b) illuminates the objects with separate radar bursts, creating separate returns and resolving the two objects.

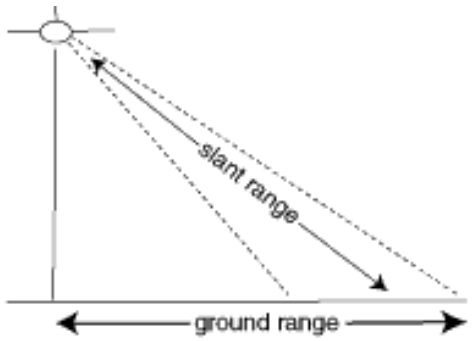

Figure 3.5: Slant and ground range (Campbell, 1996).

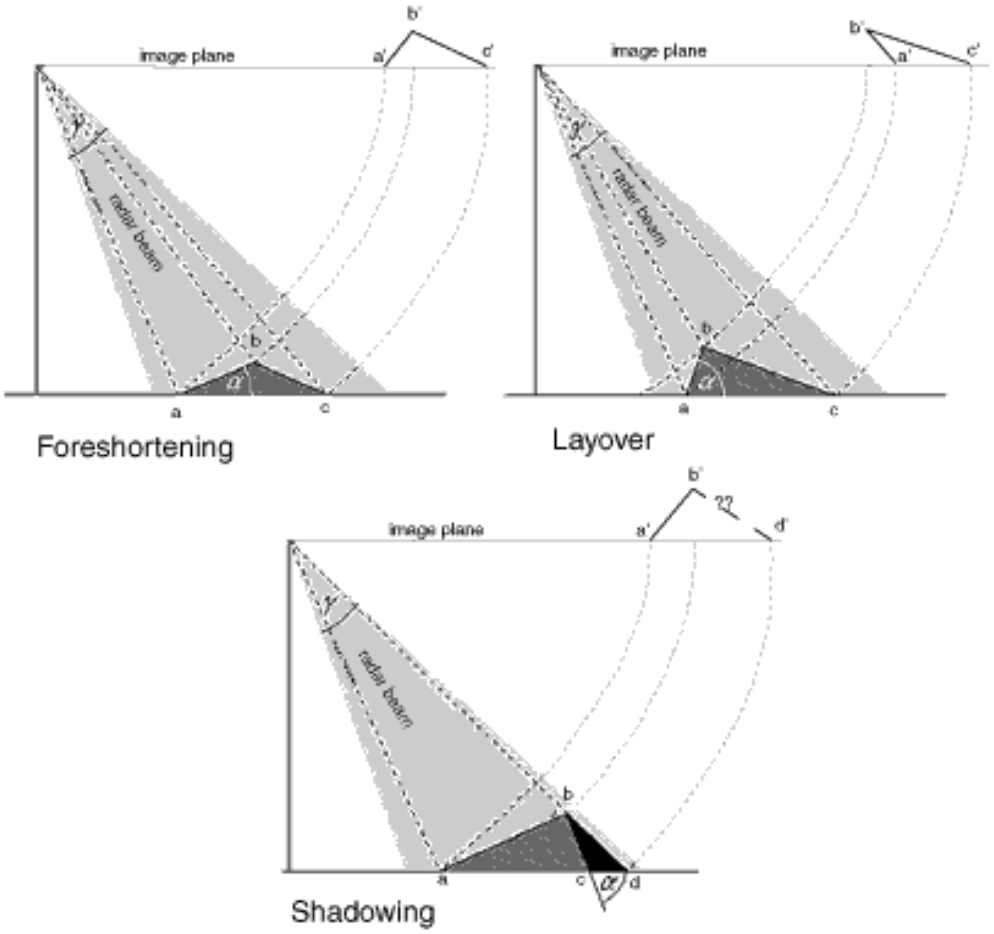

Figure 3.6: SAR geometeric distortiorn (Olmsted, 1993). Inn oreshortening, point "b" is closer to the SAR than it isisn actual ground disstnce. In layover, point "b" is closer to the SAR than poiit "a." In shadowing, , portion of the mountain is not illuminated, no data isseceived for this areae

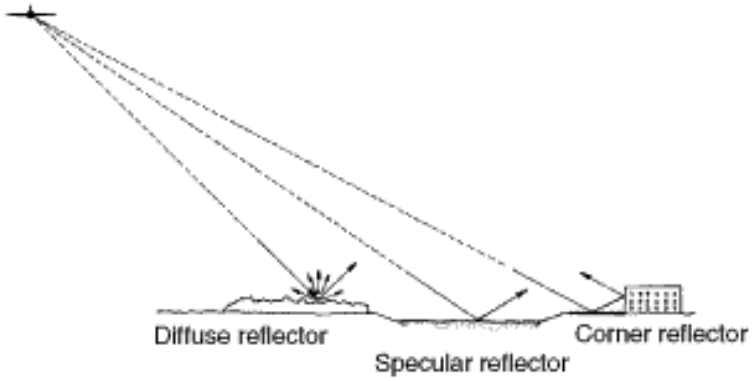

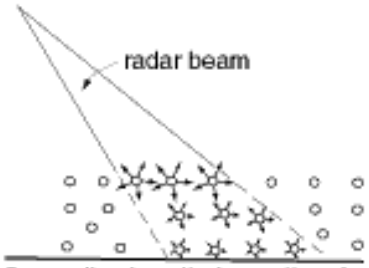

Generalized scattering pattern in a volume reflector.

Figure 3.7: Diffuse, specular, corner (Lillesand and Kiefer, 1994), and volume reflection (Ulaby et al., 1981).

34

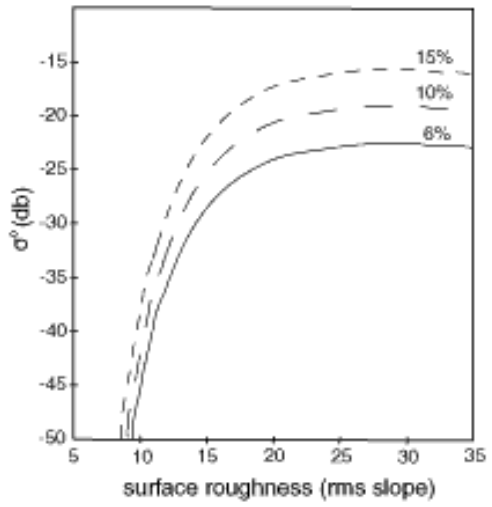

Figure 3.8: Simulated σ^{o} curves for three wet snowpacks (liquid water contents: 6, 10, and 15%), using a geometric optics model of radar backscattering (SAR average incidence angle 12°). Increased backscattering is associated with increased surface roughness. Surface roughness is parametrized as the root-means-square slope of the surface (Smith et al., 1997).

36

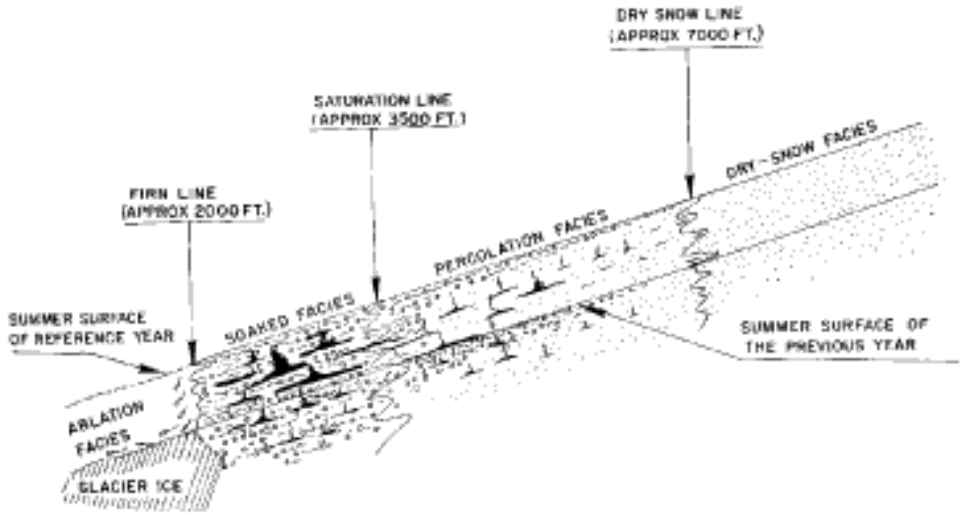

Figure 3.9: Benson's generalized cross-section of glacier facies (Benson, 1962).

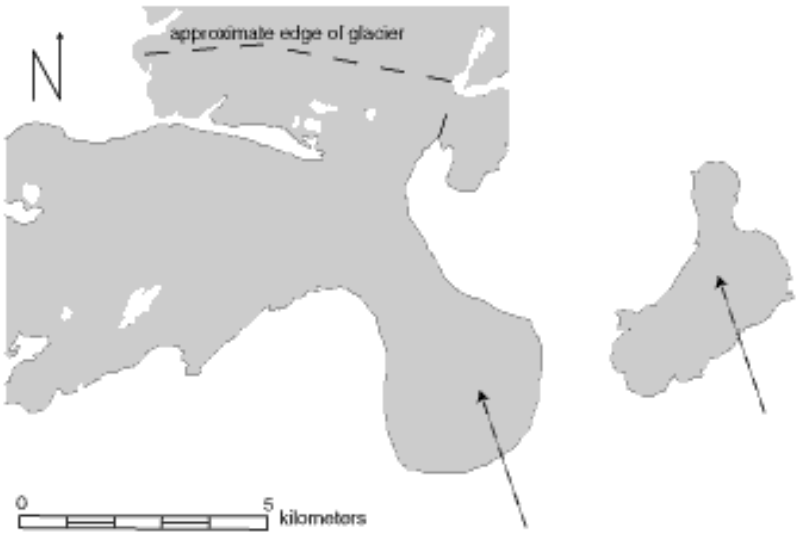

Figure 4.1: ERS-2 and Radarsat look angles (dashed arrows) relative to Commonwealth and Howard Glaciers. Orientations and scale correct but positions are arbitrary.

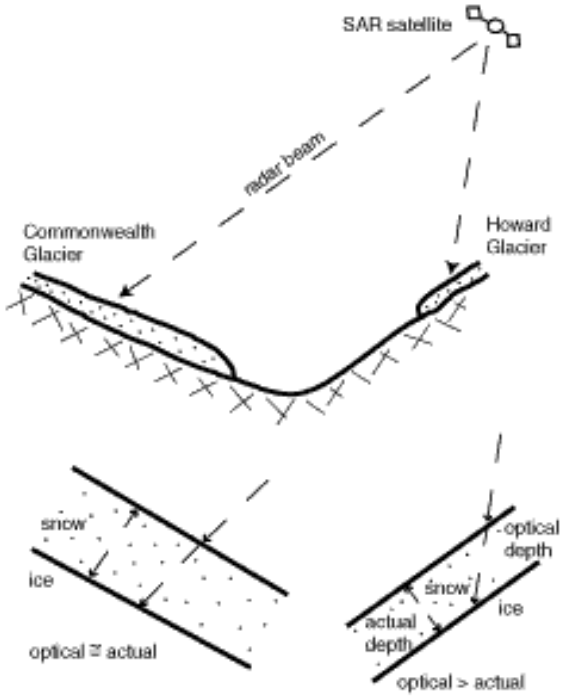

Figure 4.2: Optical depth vs. actual depth.

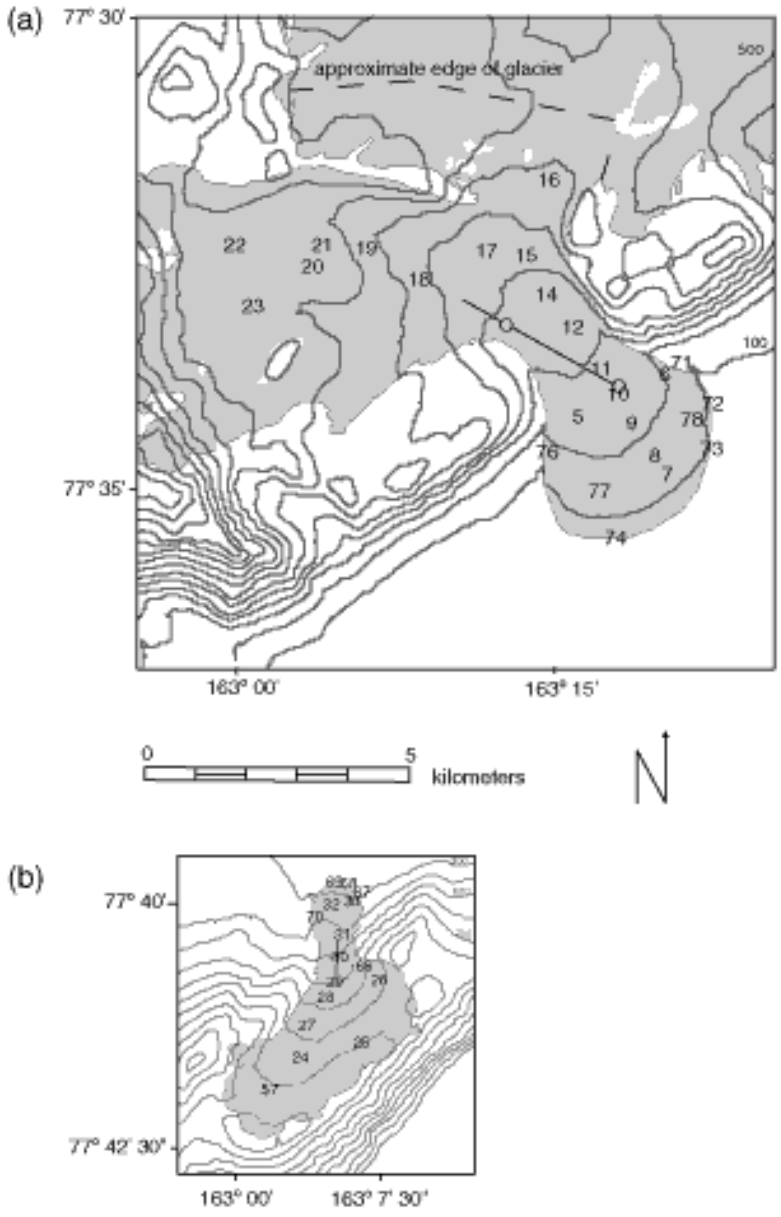

Figure 4.3: Snow stakes on (a) Commonwealth and (b) Howard Glaciers. Numbers indicate snow stake location, lines are transect locations, and contour interval 100 m.

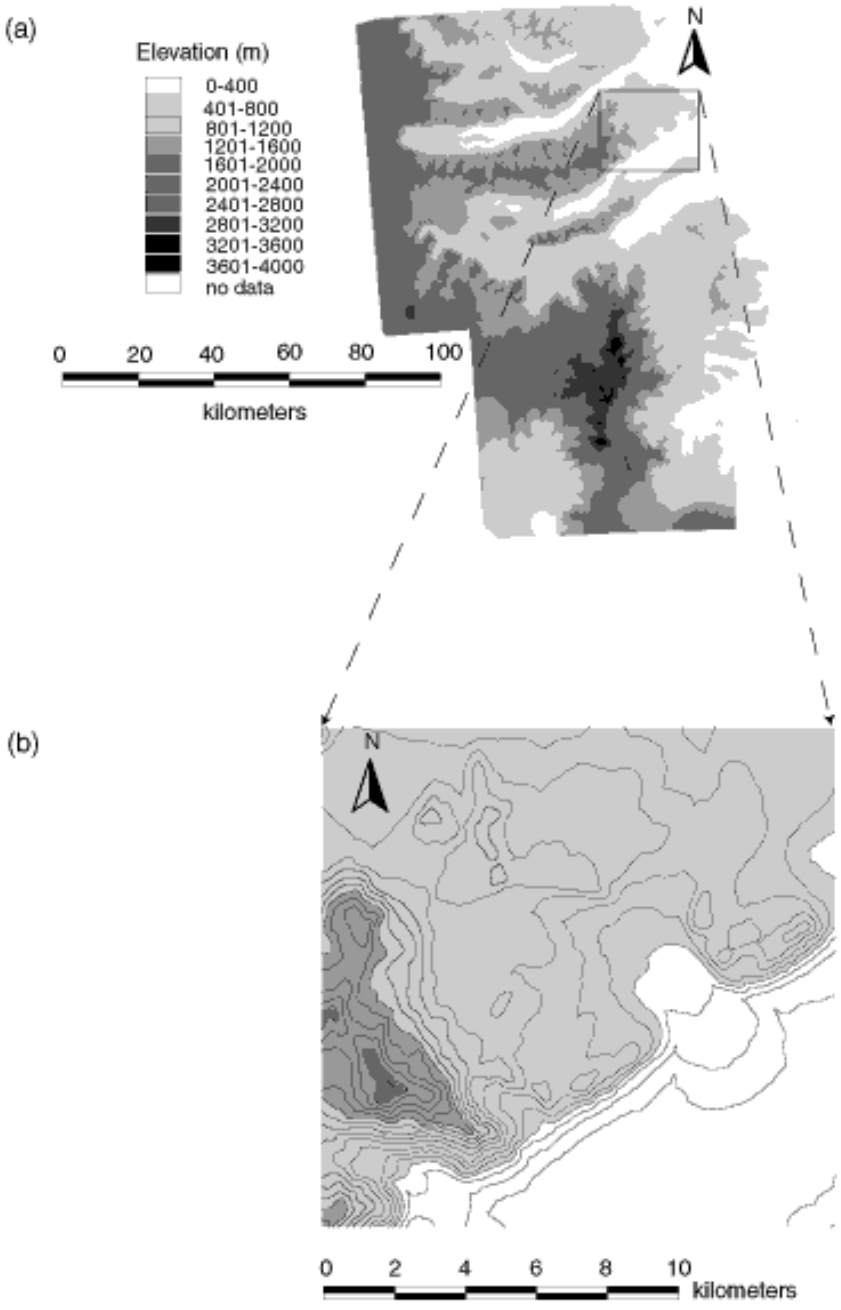

Figure 4.4: A visual representation of the digital elevation model of (a) Southern Victoria Land, Antarctica. (b) Commonwealth Glacier and surrounding area. Contour interval 100 meters.

47

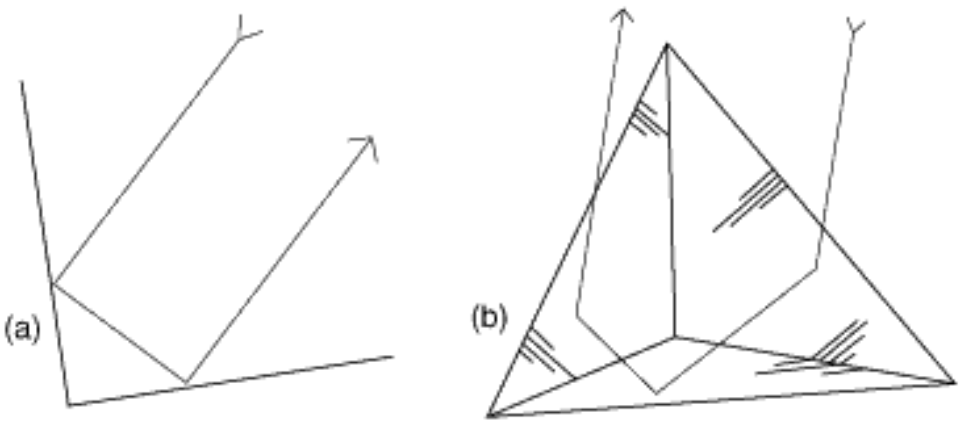

Figure 4.5: (a) A ray diagram of the reelection in a dihedraaborner reflector. (bb) A ray diagram of the reflection in a triaiagular trihedral conrer reflector (Fuller,r, 1970).

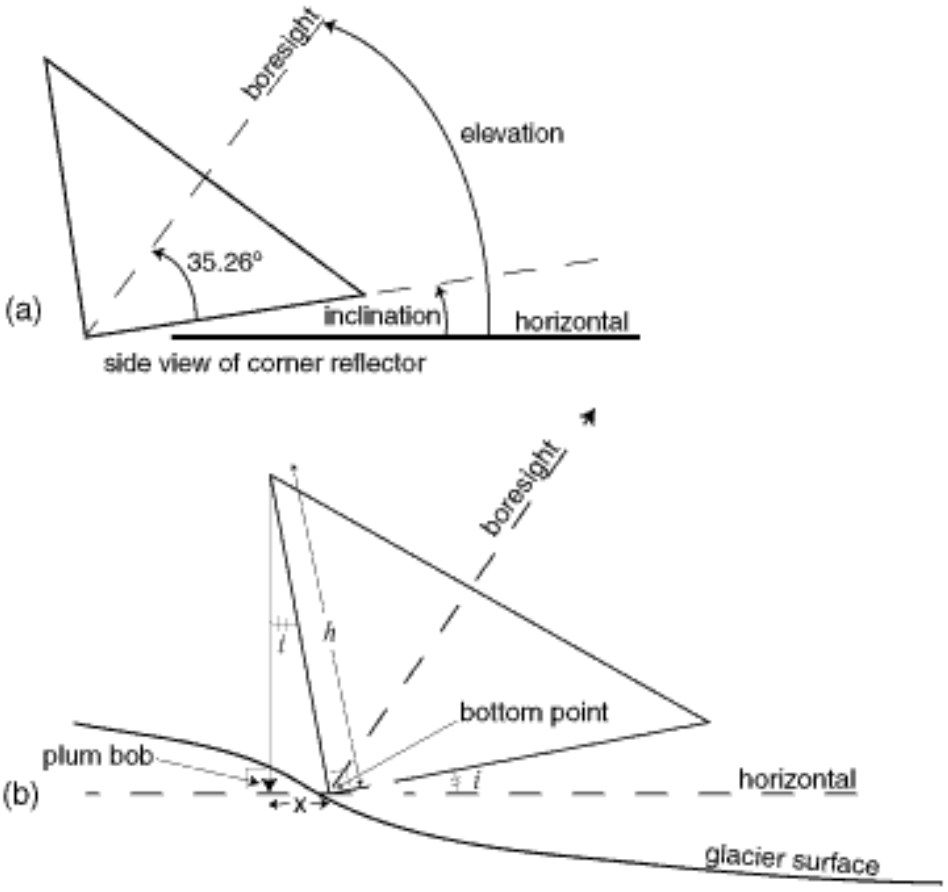

Figure 4.6: (a) Inclination angle (ASF website). (b) Determining the inclination angle.

Figure 4.7: A trihedral corner reflector.

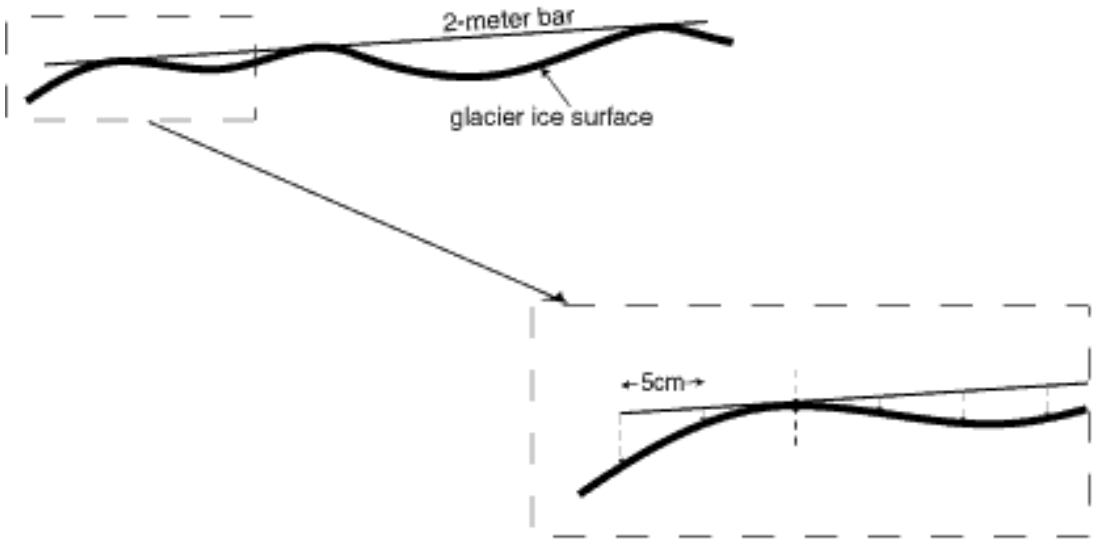

Figure 4.8: Ice surface roughness measured from a 2 m bar to ice surface.

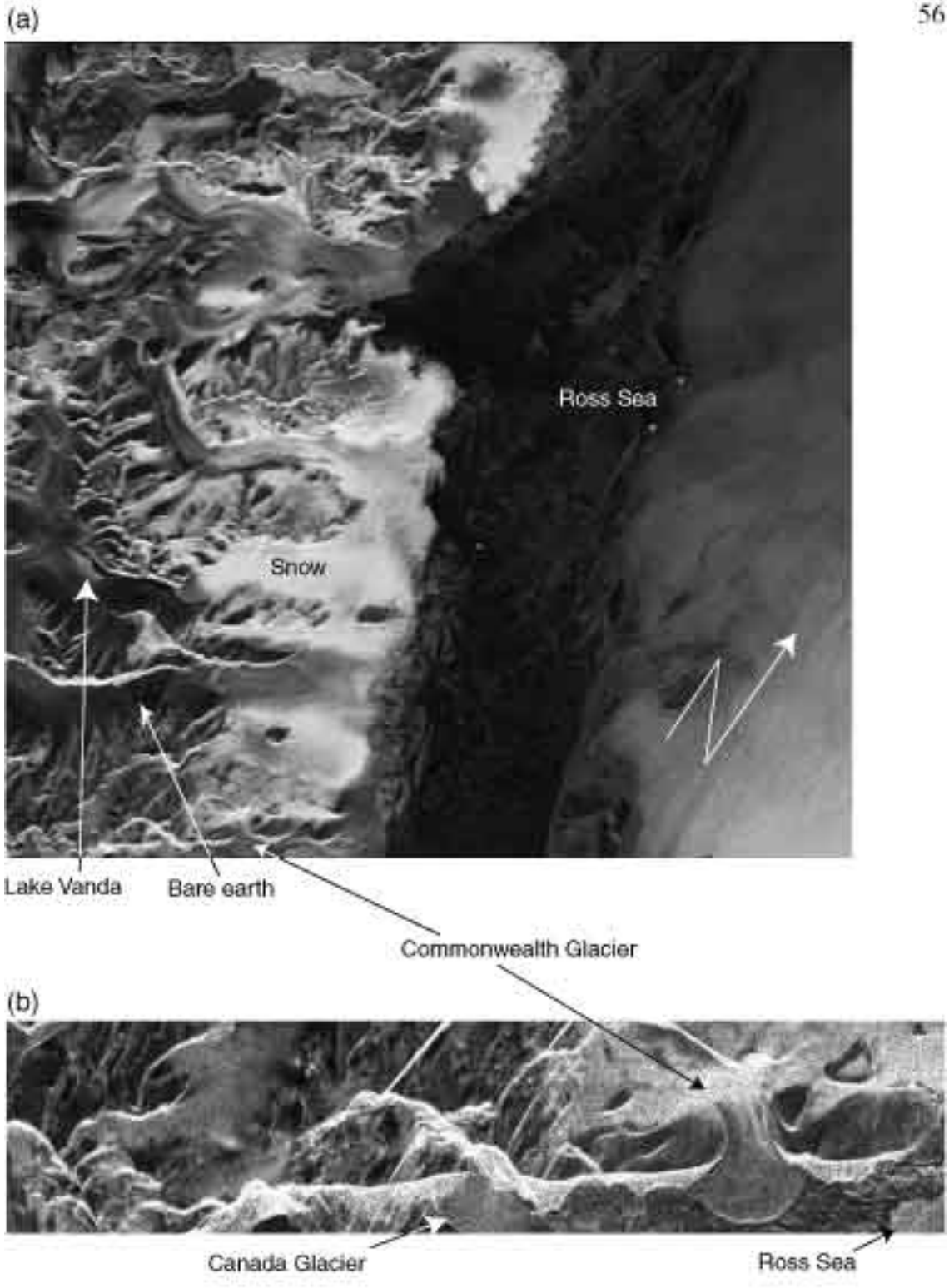

Figure 5.1: ERS-2 uncorrected SAR: (() full scene, (b) deetil of portion of Taylor Valley. Images ©1999 European Space Agency.

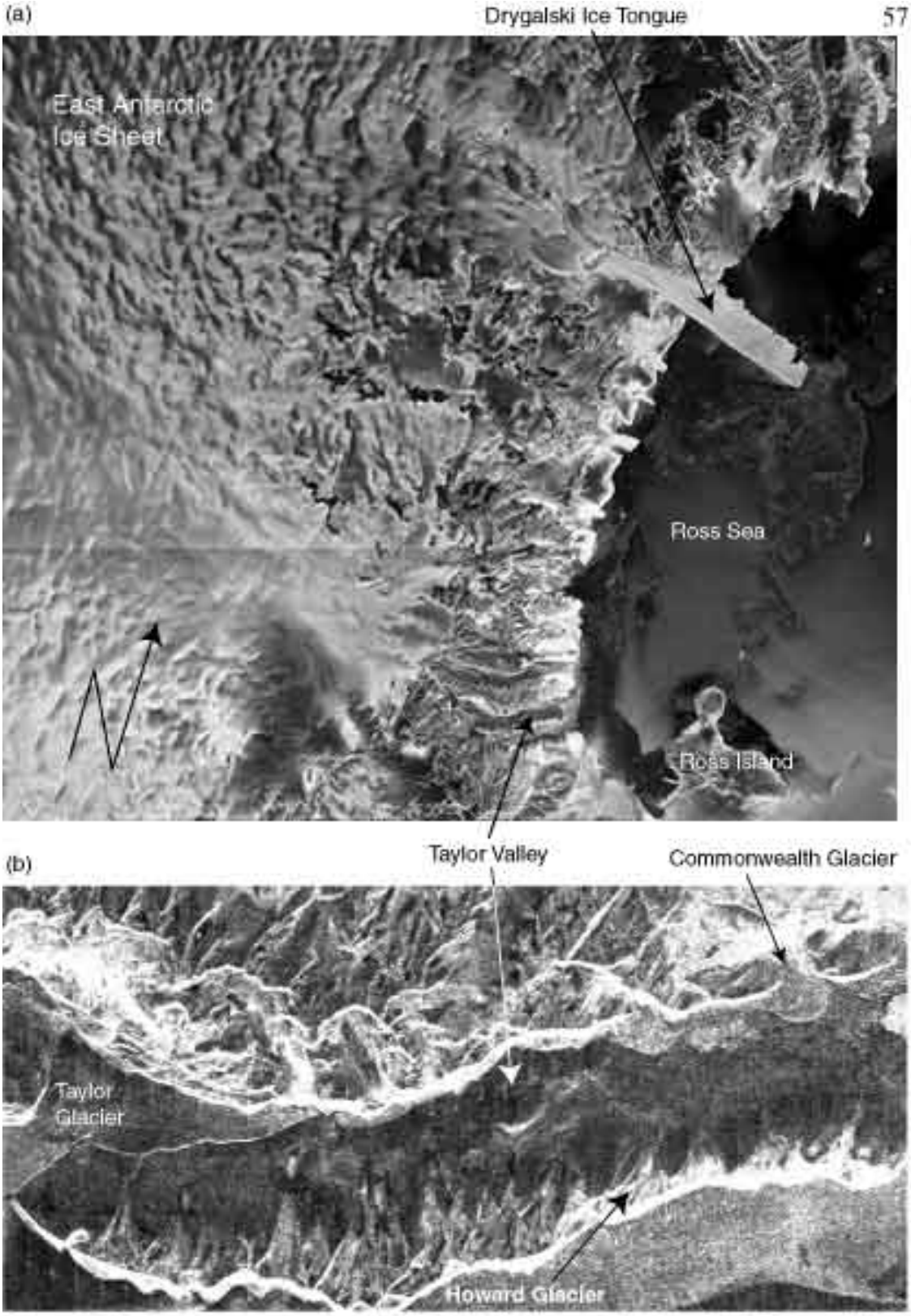

Figure 5.2: Radarsat uncorrected SAR: (a) full scene, (b) detail of Taylor Valley. Image ©1999 Canadian Space Agency.

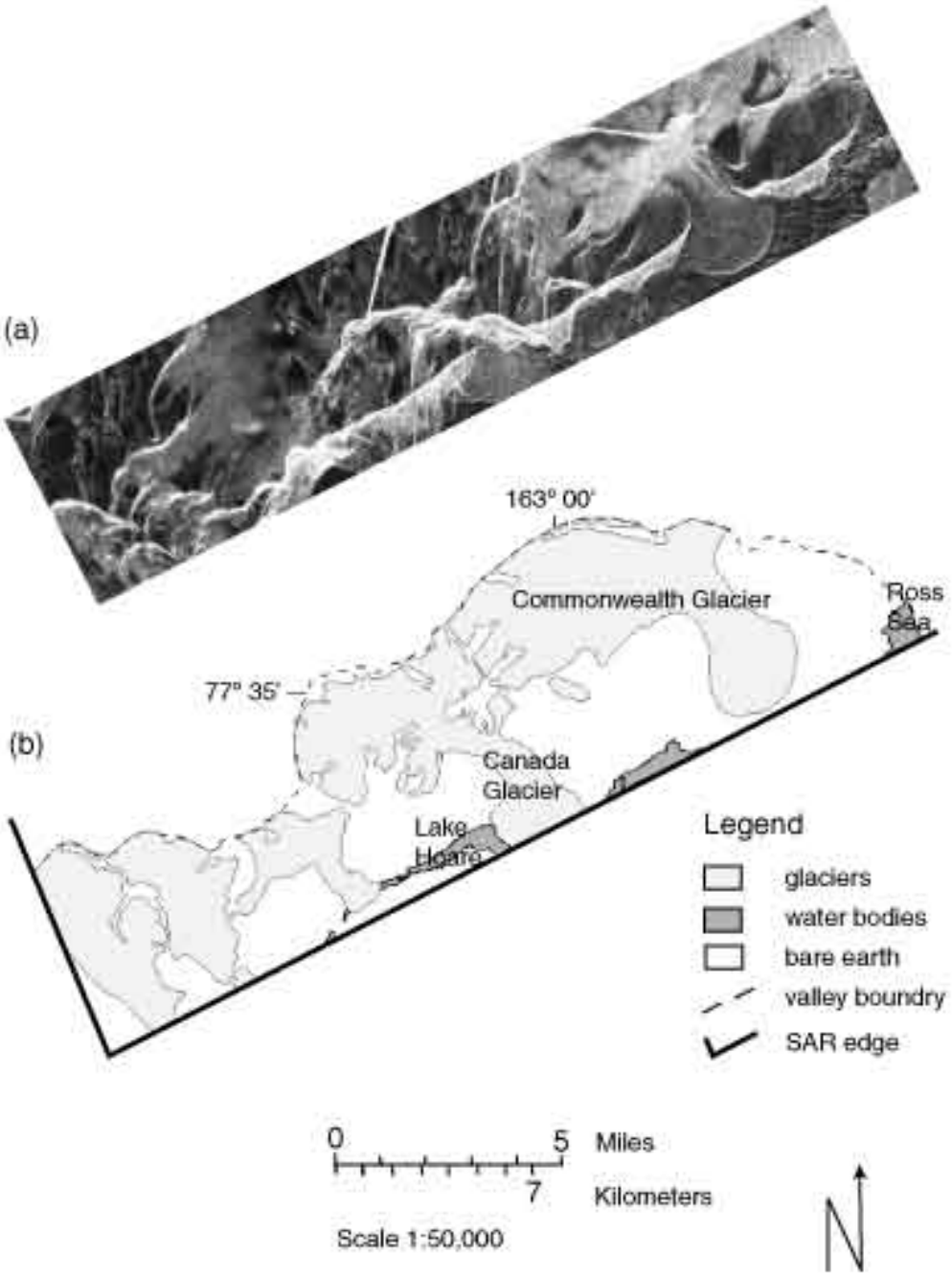

Figure 5.3: The portion of Talor Valley that was imaged by the ERS-2 SAR (a) uncorrected SAR, (b) map.

61

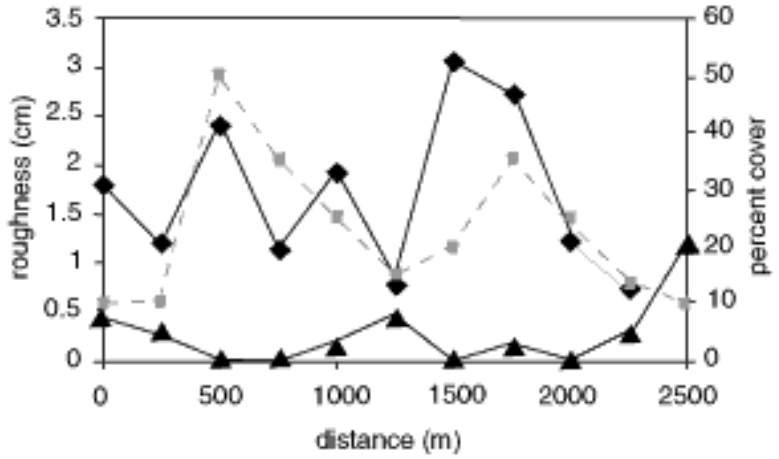

Figure 5.4: Surface characteristics aloog the transect on C Ommonwealth Glacier. Standard deviation of roughnɛss is indicated by tlth black diamonds. . Snow tables (given as percentage of ɛ æea cover) are indicicted by gray squares and dashed lines. Cryoconite:ɐioles (also presentntd as percentage of area cover) are indicated by black t tangles.

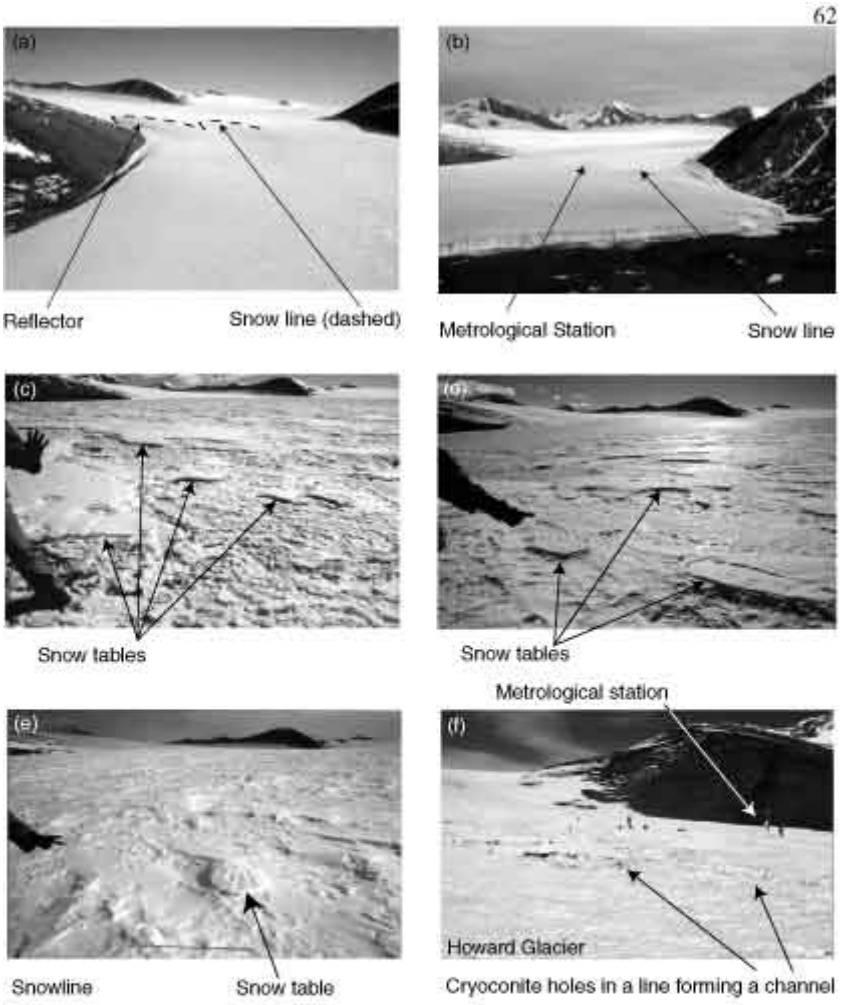

Figure 5.5: Hand-held photographs of Commonwealth (a-e) and Howard (f) Glaciers. (a) West side of snowline from helicopter 300-500' above ground level taken January 20, 1999 looking approximately NNW. (b) East side of snowline from helicopter looking approximately West (same date and flying height as (a)). (c) Site 4 on transect, looking NW. (d) Site 6 on transect, looking NW. (e) Above snowline at site 12 on transect looking NW. (d) Cryoconite hole channel on Howard Glacier in ablation area. Photos a,c,d,e © 1999 Patrick J. Bardel, b,f © 1999 Andrew G. Fountain.

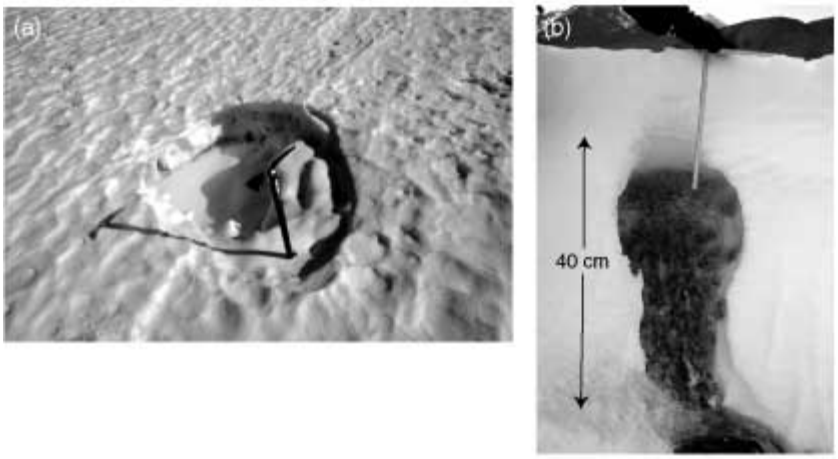

Figure 5.6: Cryoconite hole (a) top view with ice axe for scale, (b) side view of cannibalized hole on side of cliff.

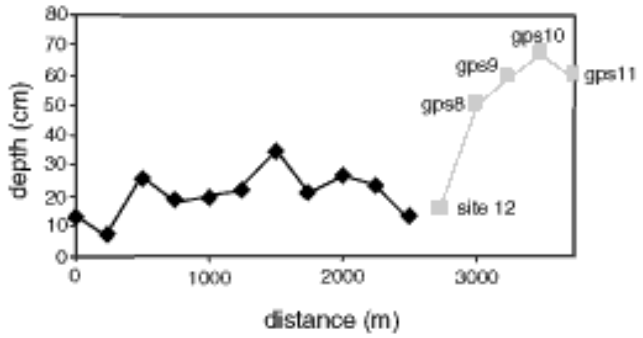

Figure 5.7: Snow depths along the transect on Commonwealth Glacier. Black diamonds are averaged snow depths on snow tables in the ablation area; gray squares are averaged depths in the accumulation area.

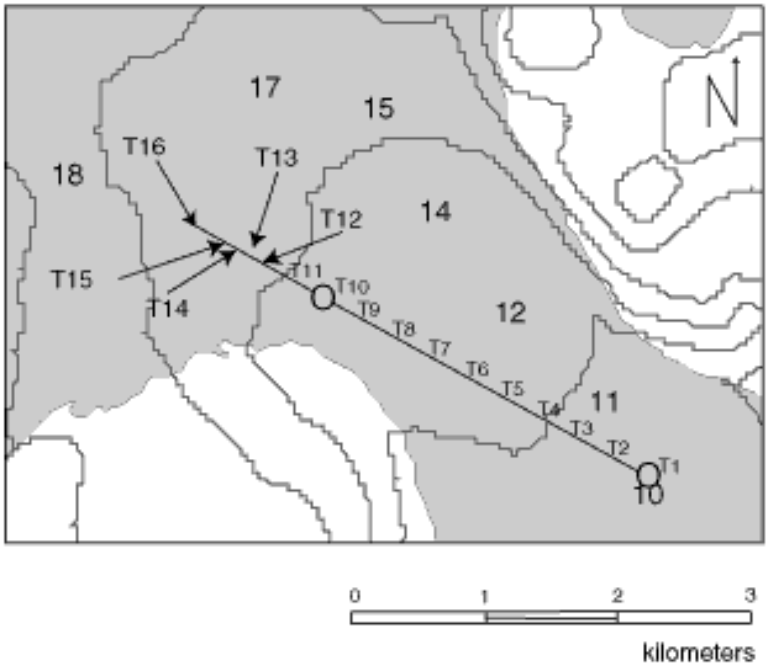

Figure 5.8: Snow stakes (numbers), radar reflectors (circles), transect route (line), and sample sites (T1-T16) on Commonwealth Glacier. Location of sample sites are where label touches transect line, at arrow point, or at center of reflector location circle. Contour interval 100 m.

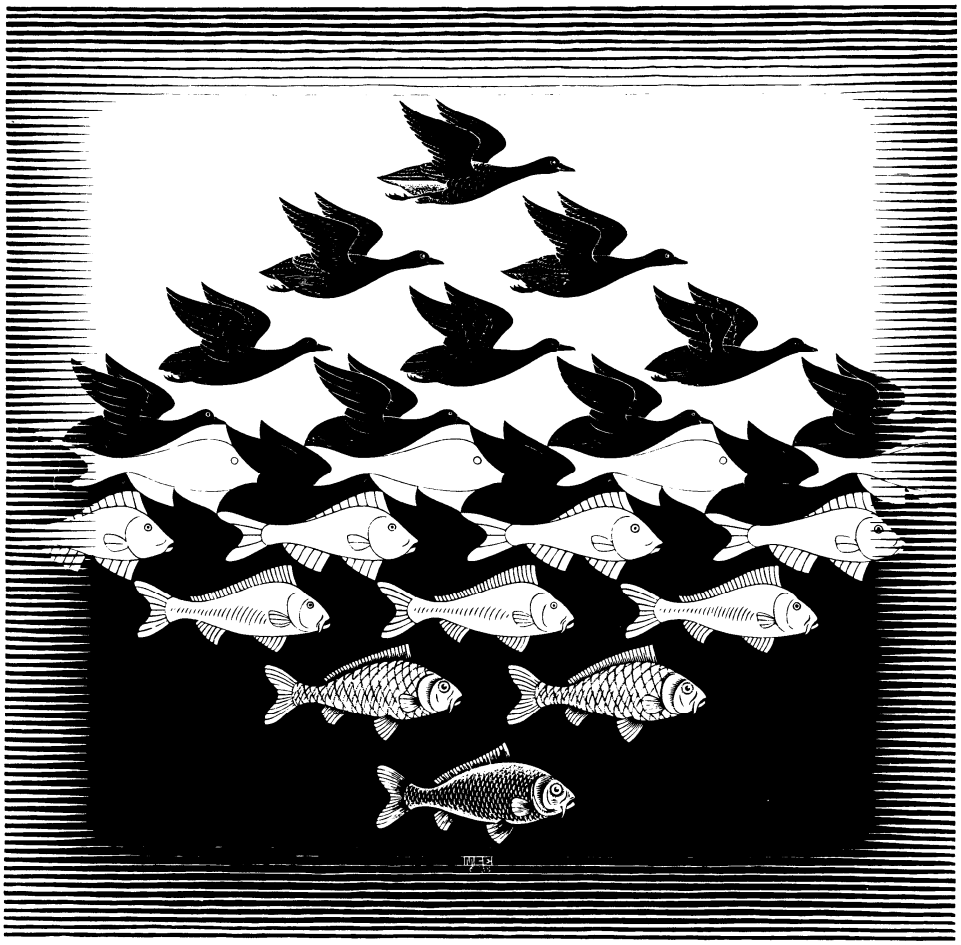

Figure 5.8 Sky and Water I

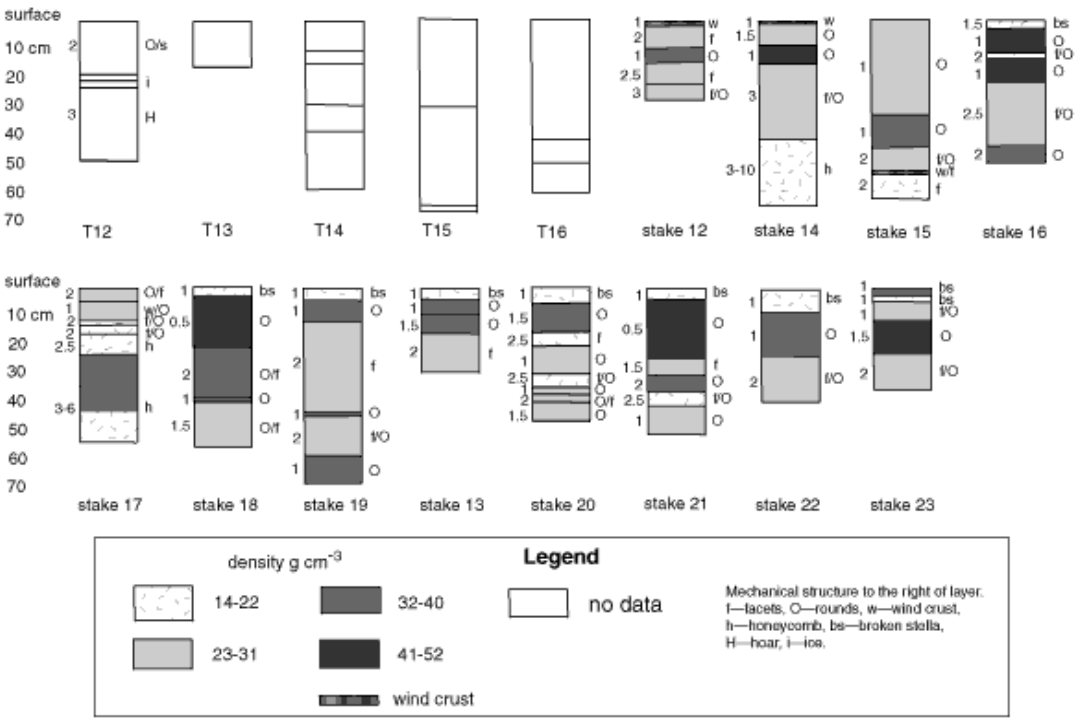

Figure 5.9: Snow layers graph. Grain size (mm) to the left of layer. Numbers to the far left indicate depth of layers.

67 99

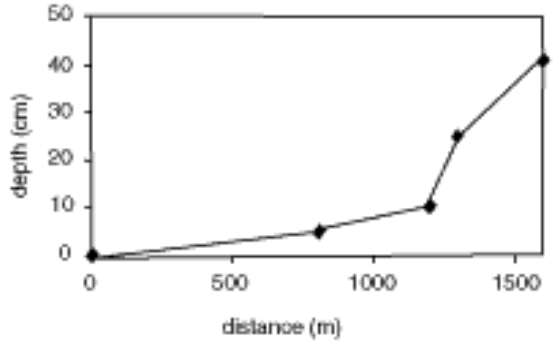

Figure 5.10: Averaged snow depths along the transect on Howard Glacier. Snowline located at third data point at 200 m.

72

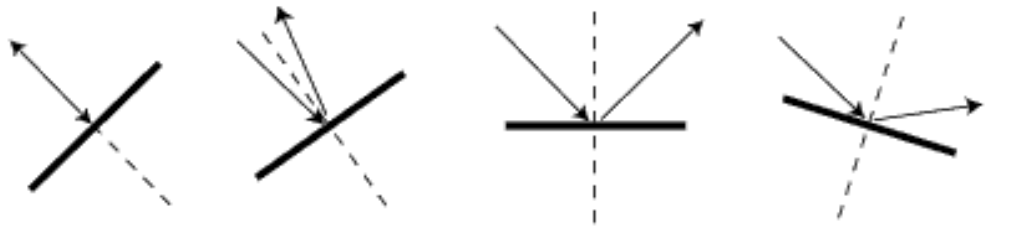

Figure 6.1: Effect of a SAR beam scattering off specular surfaces of different incidence angles (ASF website).

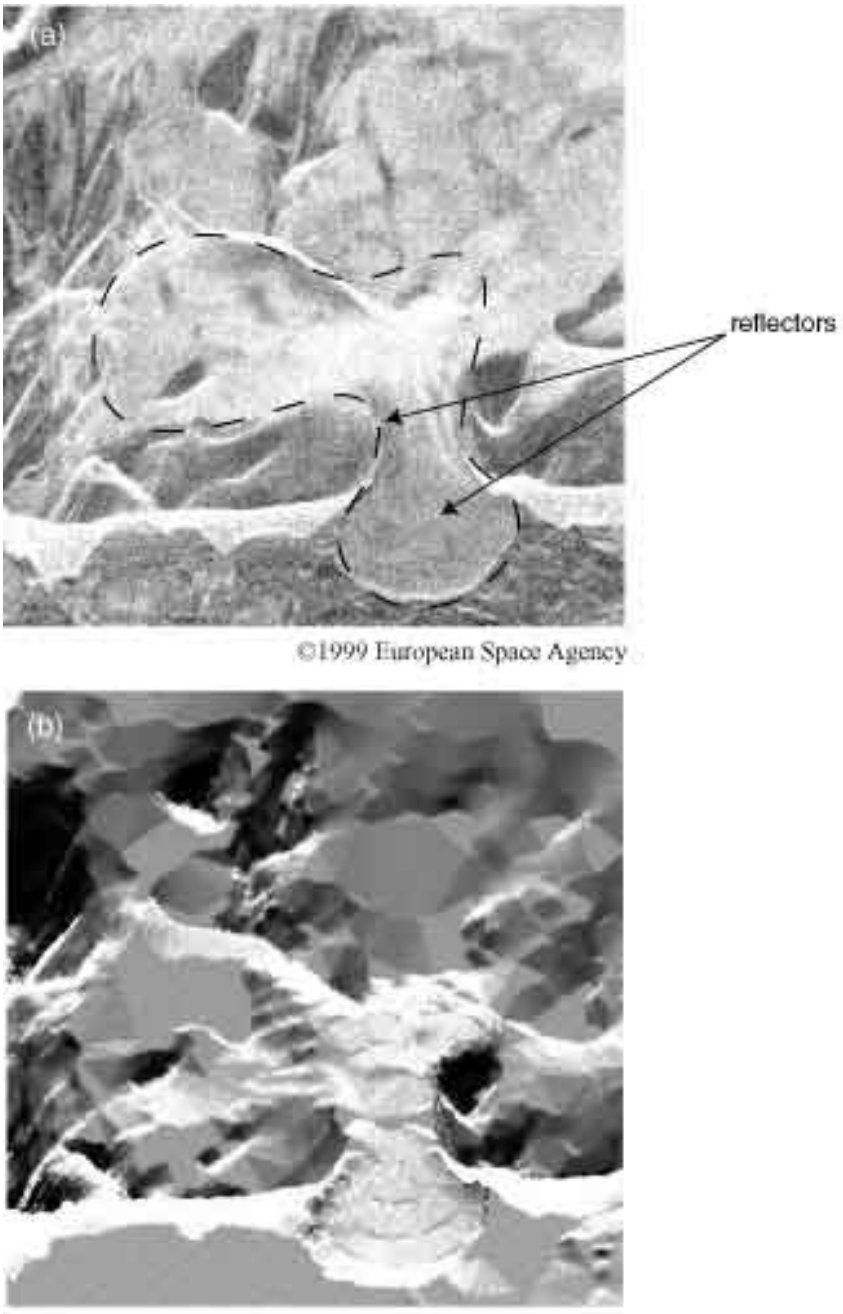

Figure 6.2: Intermediate terrcorr images of Commonwealth Glacier and surrounding area. (a) Preprocessed SAR image. Approximate outline of glacier shown in dashed line. (b) Simulated SAR image. The image is "blocky" because it is created from the 30 m resolution DEM.

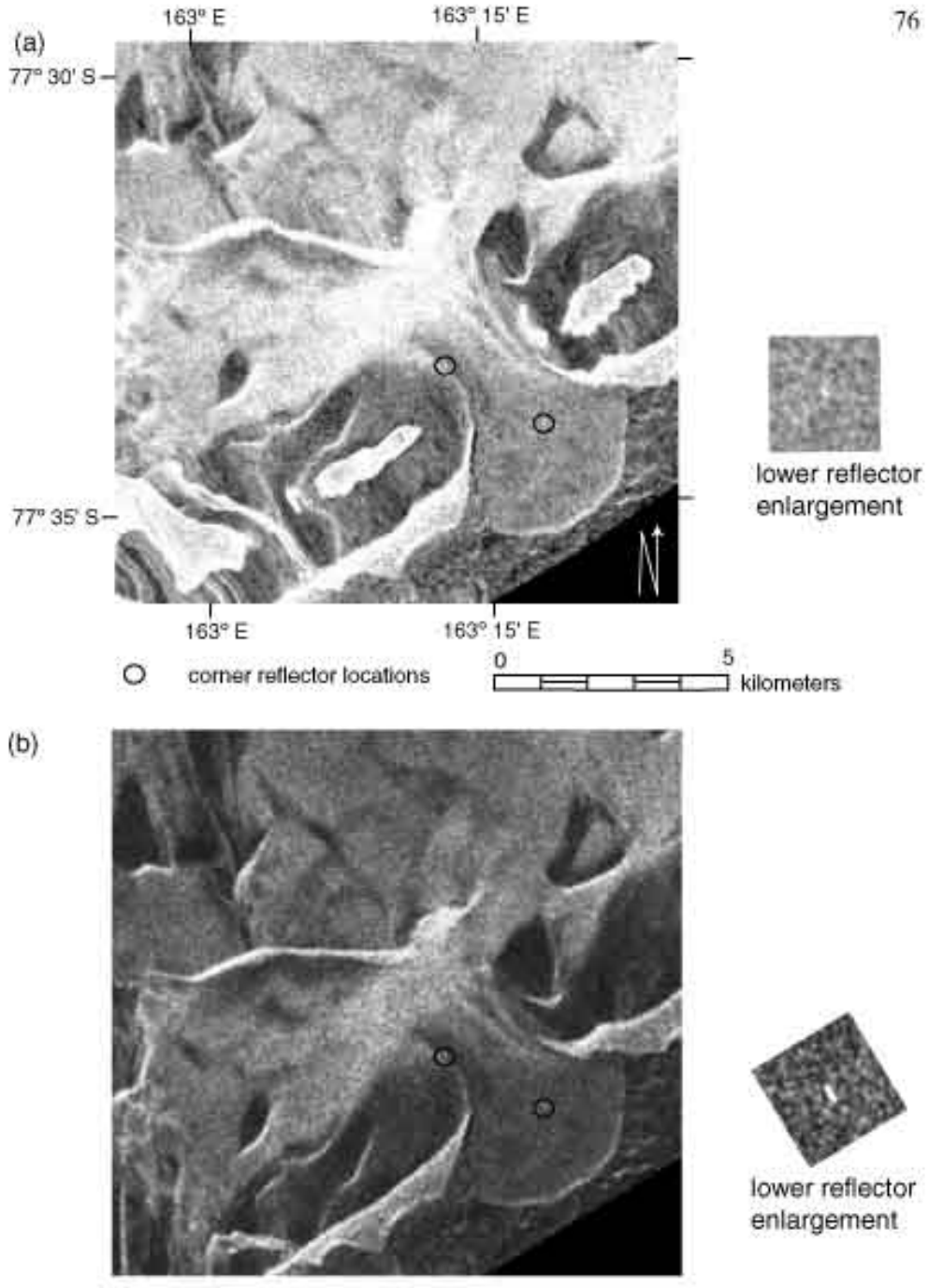

Figure 6.3: Auto terrain corrected (a) and uncorrected image (b) comparison ERS-2 SAR of Commonwealth Glacier and surrounding area. Both images are approximately same scale. Both images ©1999 European Space Agency.

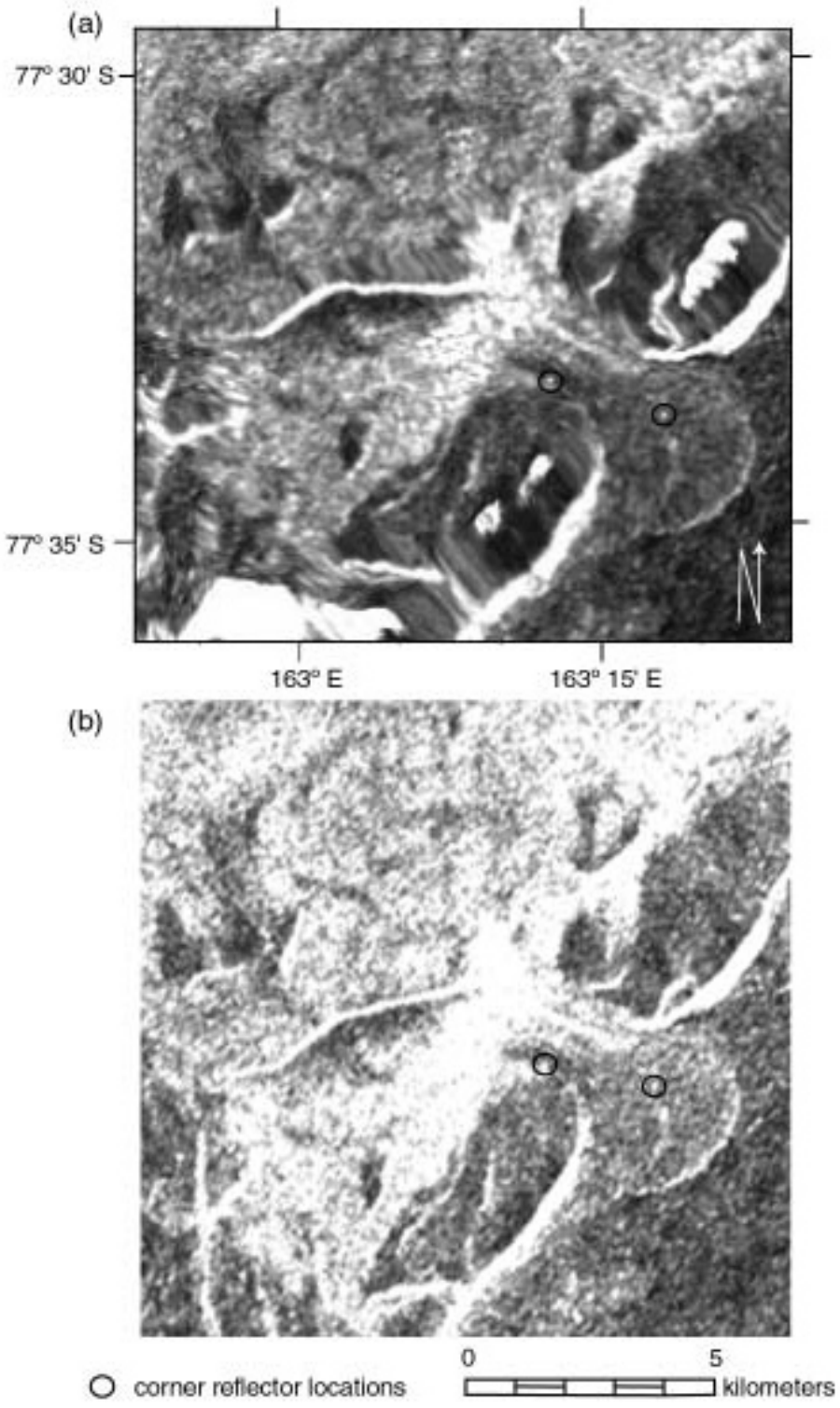

Figure 6.4: (a) Terrain corrected Radarsat ScanSAR of Commonwealth Glacier and surrounding area. (b) Uncorrected Radarsat ScanSAR of approximately same area. Scales are approximately the same. Both images ©1999 Canadian Space Agency.

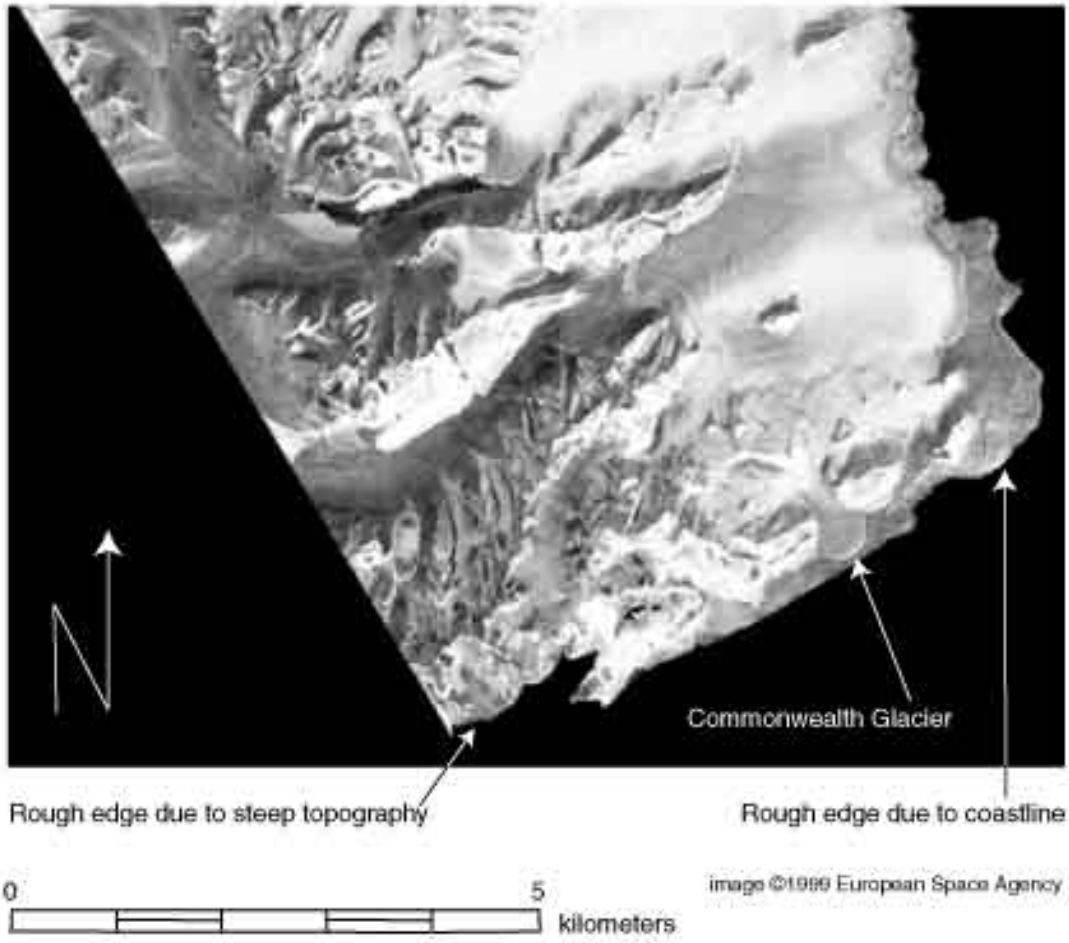

Figure 6.5: ERS-2 terrain corrected SAR.

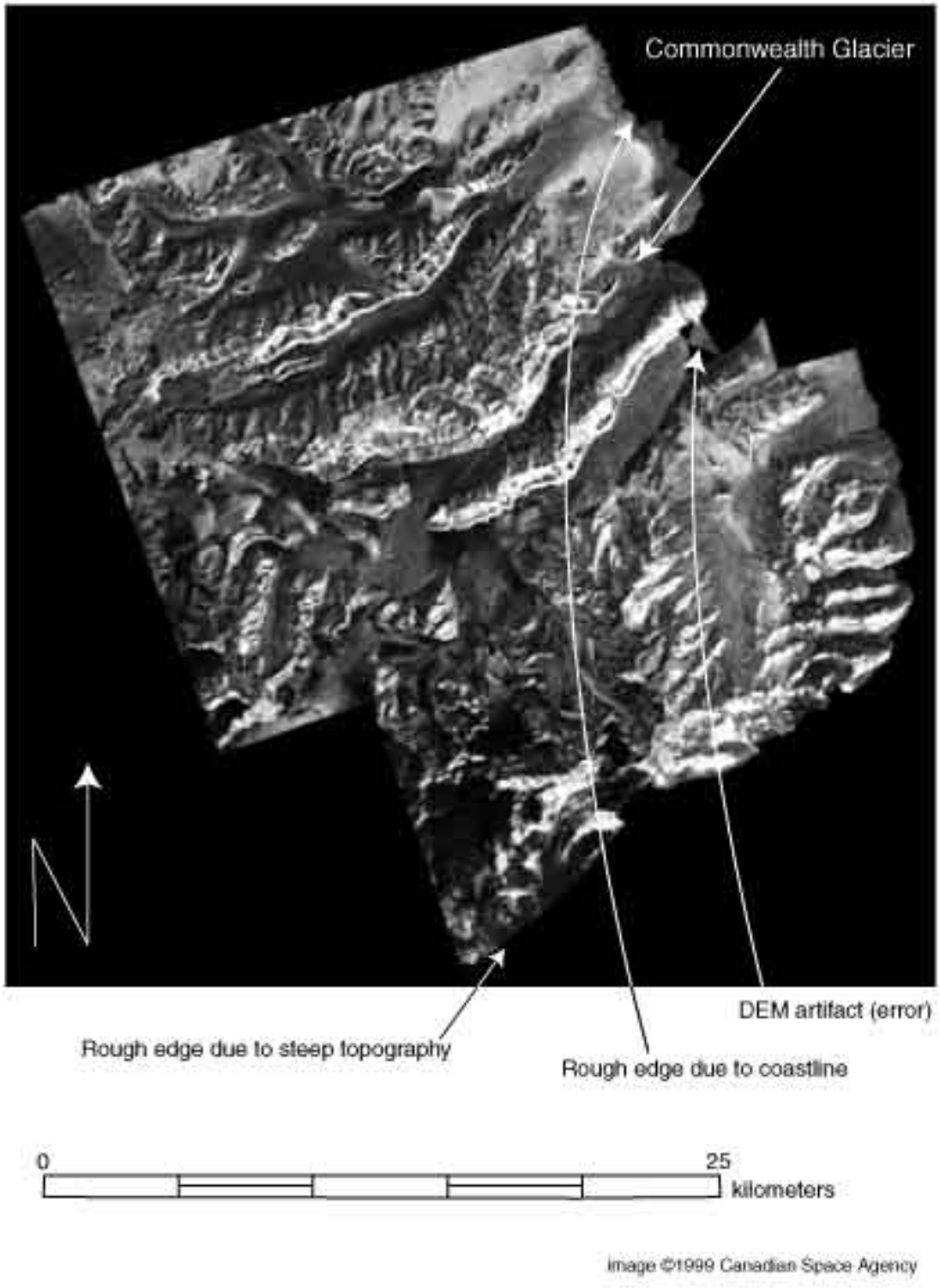

Figure 6.6: Radarsat terrain correcteddSAR.

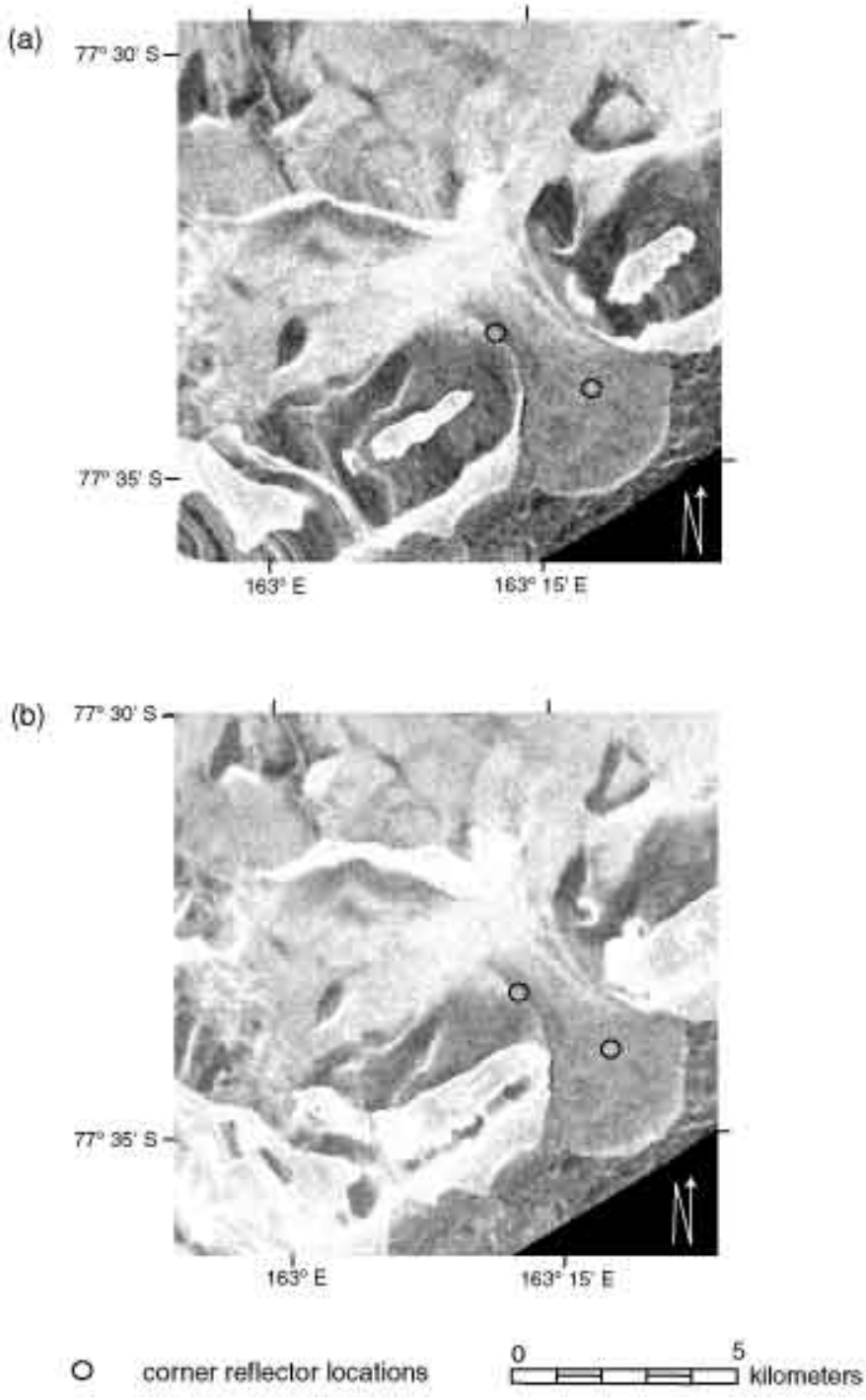

Figure 6.7: (a) Auto-correlation and (b) manual-correlation terrain correction of Commonwealth Glacier and surrounding area. Scales are approximately the same. Both images ©1999 European Space Agency.

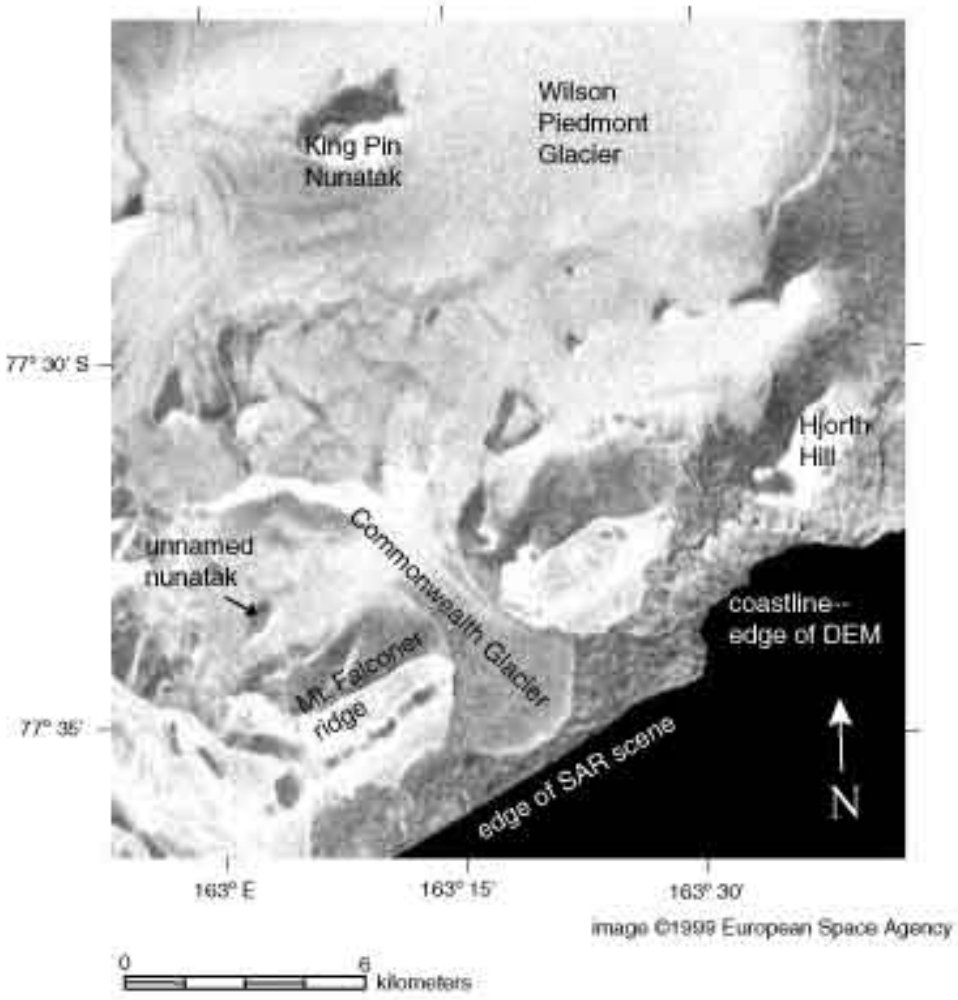

Figure 6.8: ERS-2 SAR of Commonwealth Glacier and suuounding area.

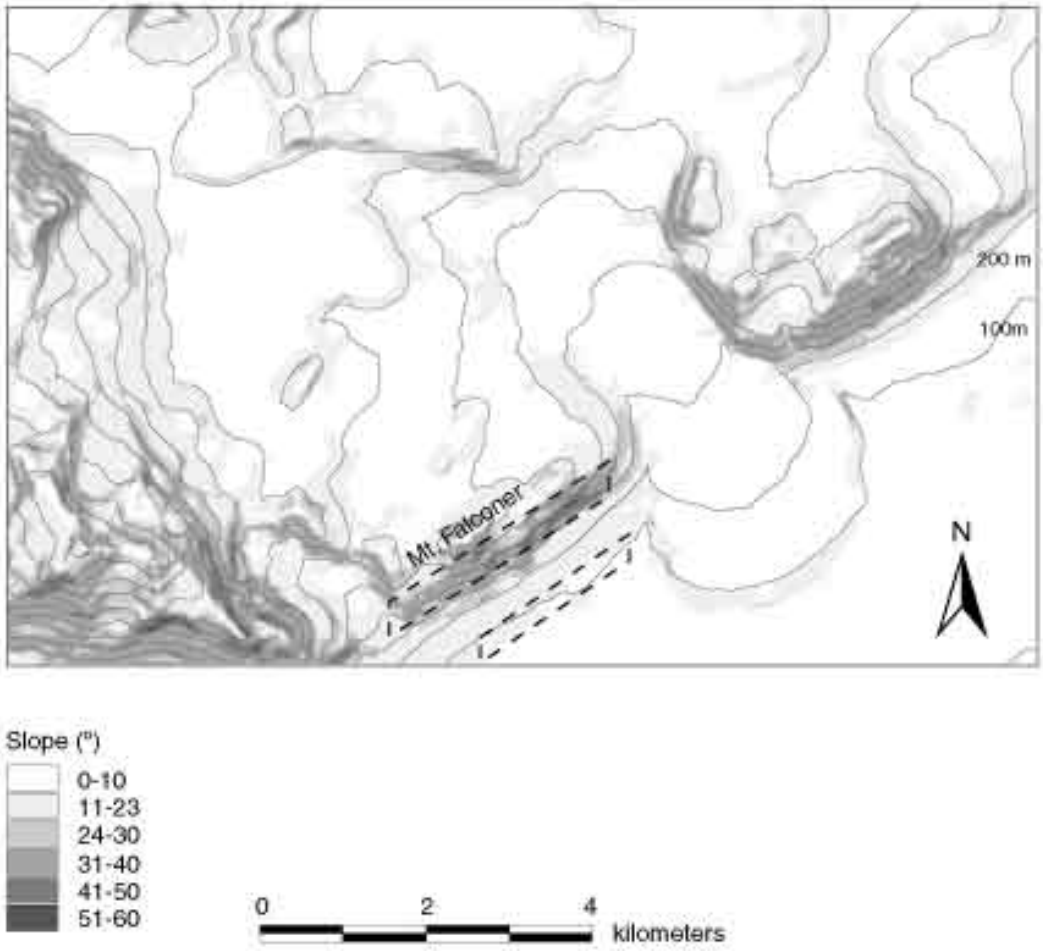

Figure 6.9: Slope and elevations (from DEM) of Commonwealth Glacier. Dashed box indicates the two bright bands on the manually corrected ERS-2 SAR image.

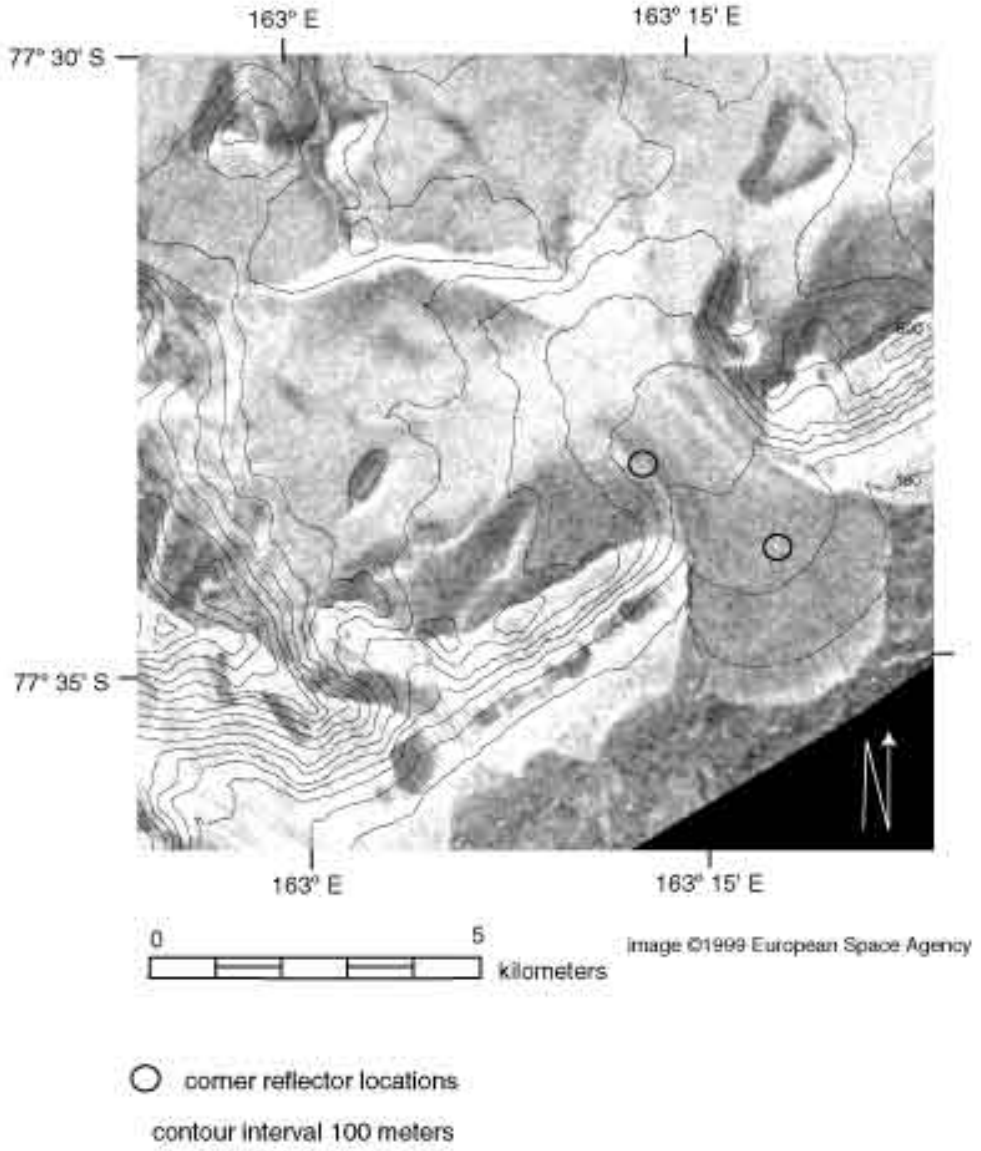

Figure 6.10: ERS-2 manually-correlated SAR image of Commonwealth Glacier with elevation contours.

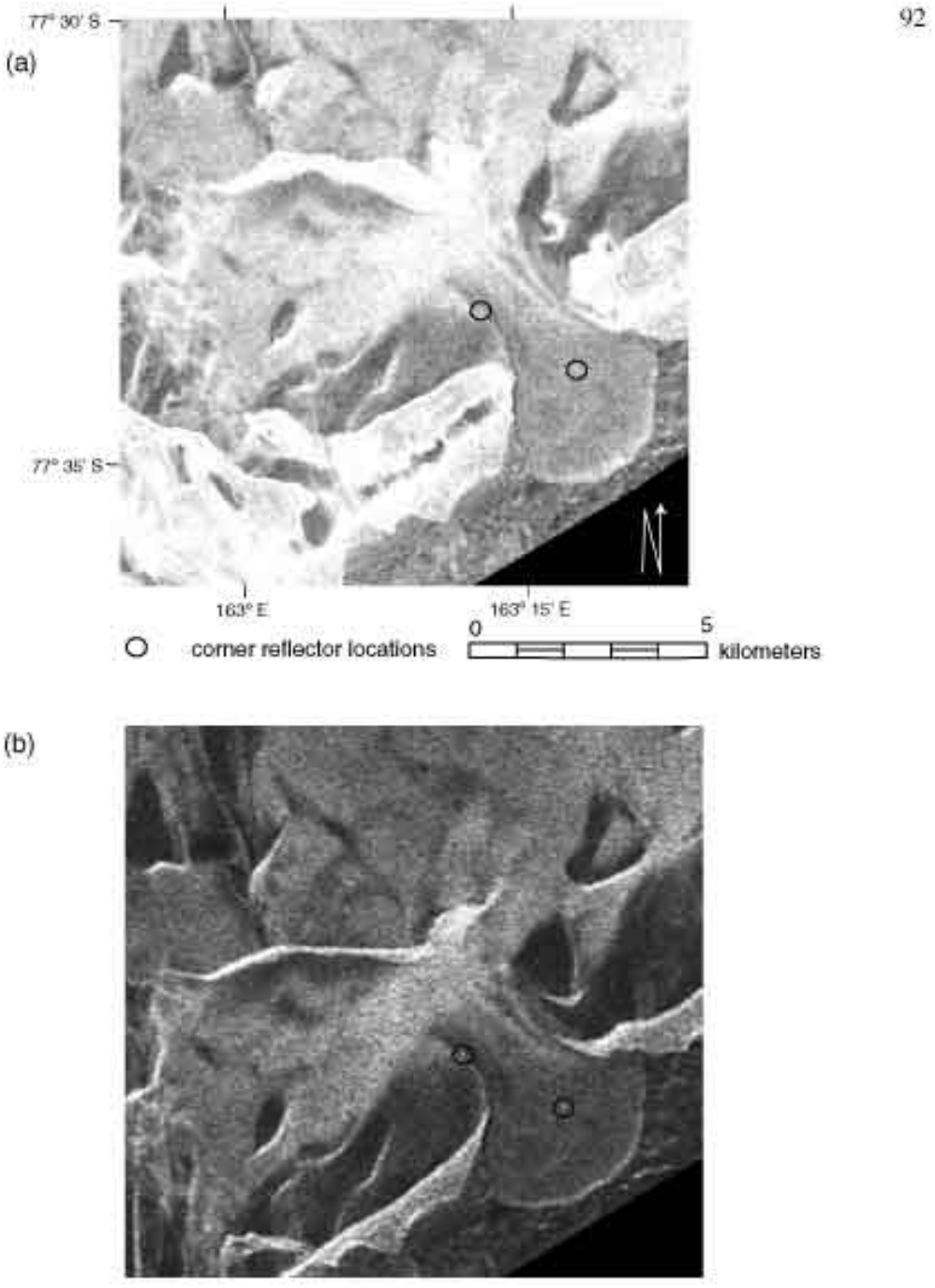

Figure 6.11: (a) Manually-correlated and (b) uncorrected ERS-2 SAR of Commonwealth Glacier and surrounding area. Both images are approximately same scale. Both images ©1999 European Space Agency.

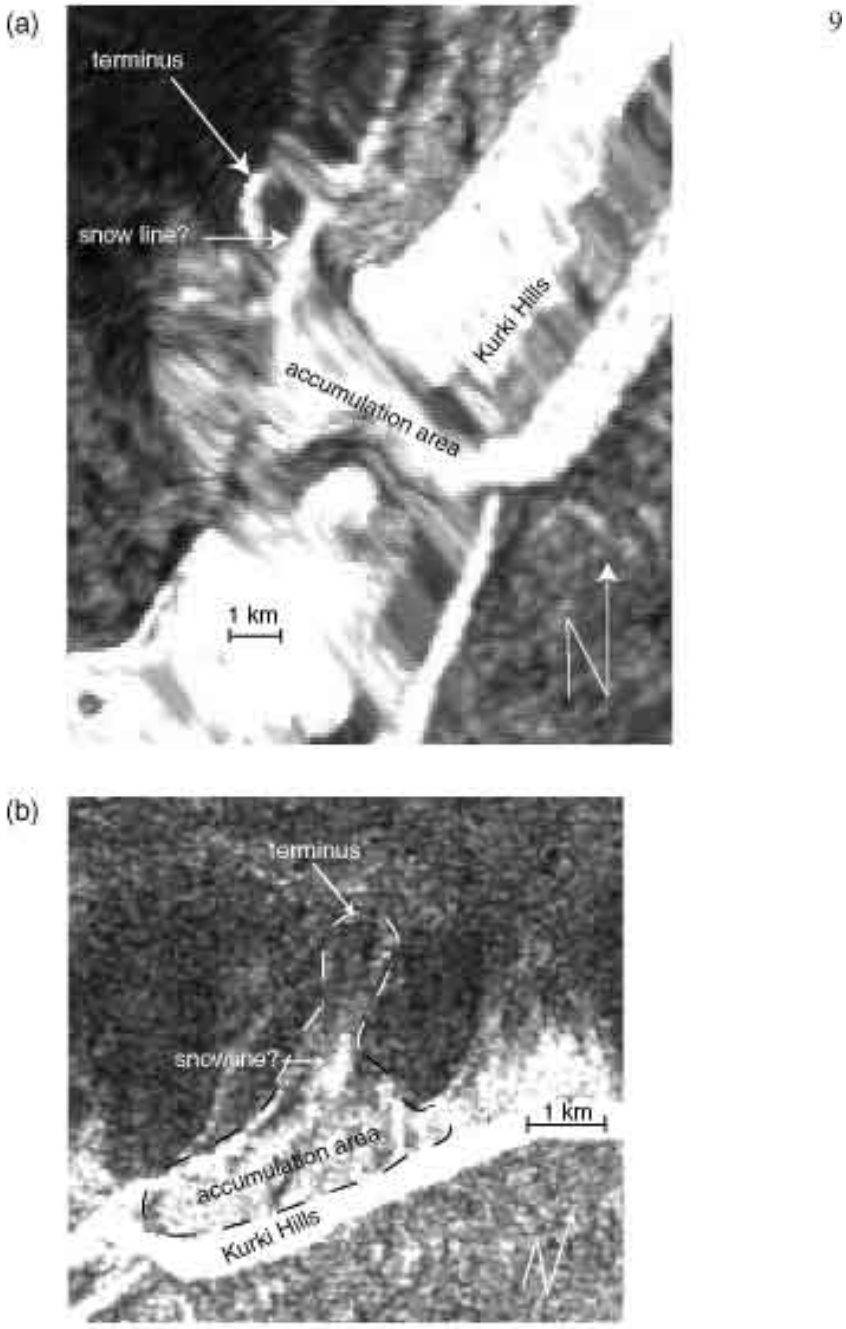

Figure 6.12: (a) Terrain corrected and (b) uncorrected Radarsat ScanSAR of Howard Glacier. Dashed line indicates approximate outline of glacier. Both images ©1999 Canadian Space Agency.

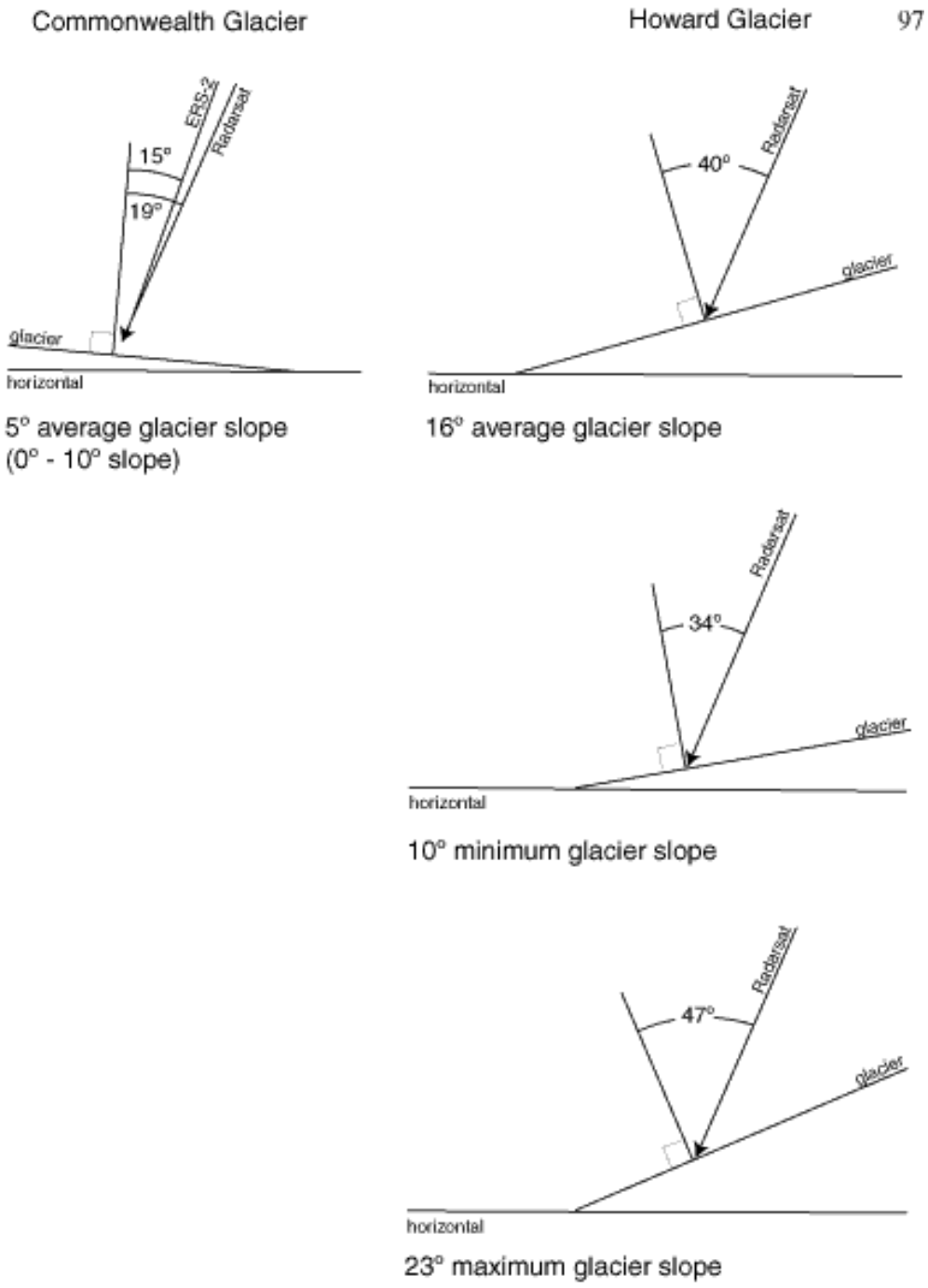

Figure 6.13: SAR local incidence angles on Commonwealth (left column) and Howard (right column) Glaciers.

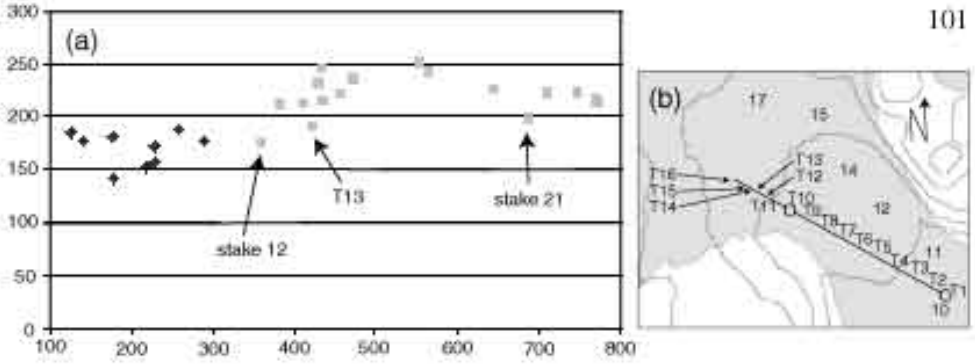

Figure 7.2: (a) SAR image brightness relative to surface elevation on Commonwealth Glacier. Black diamonds represent surfaces in the ablation area, and gray squares represent ones in the accumulation area. SAR brightness from 1/15/1999 ERS-2 terrain corrected SAR. (b) Figure 5.8 reference map.

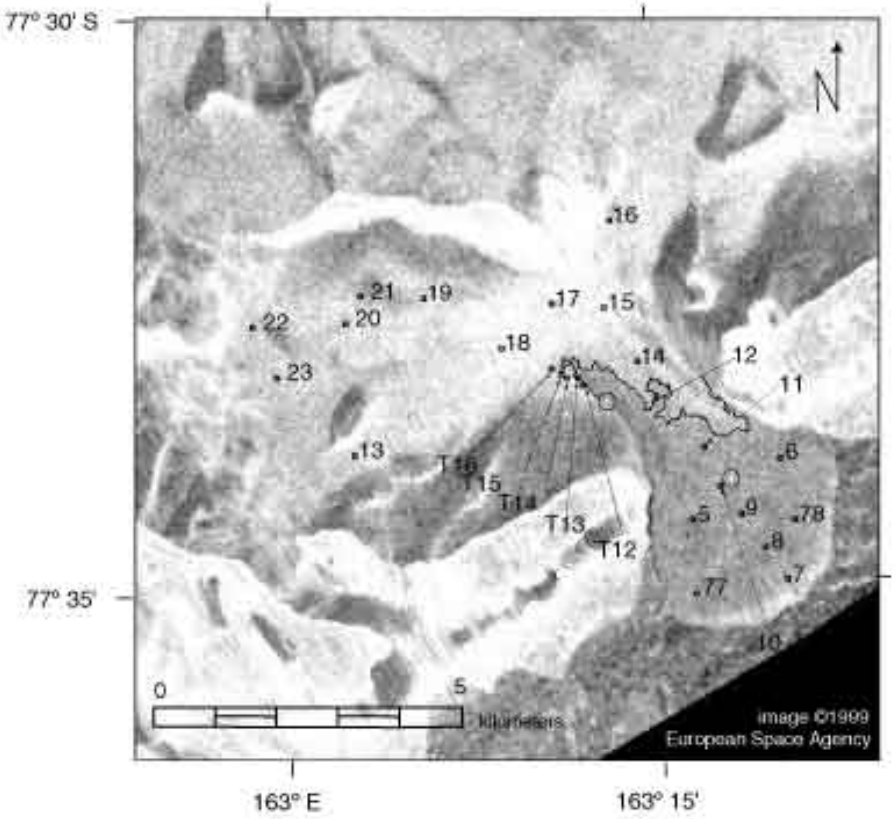

Figure 7.3: Commonwealth Glacier ERS-2 SAR 1/15/1999 snow measurement locations. Circles indicate reflector locations, and line is SAR snowline.

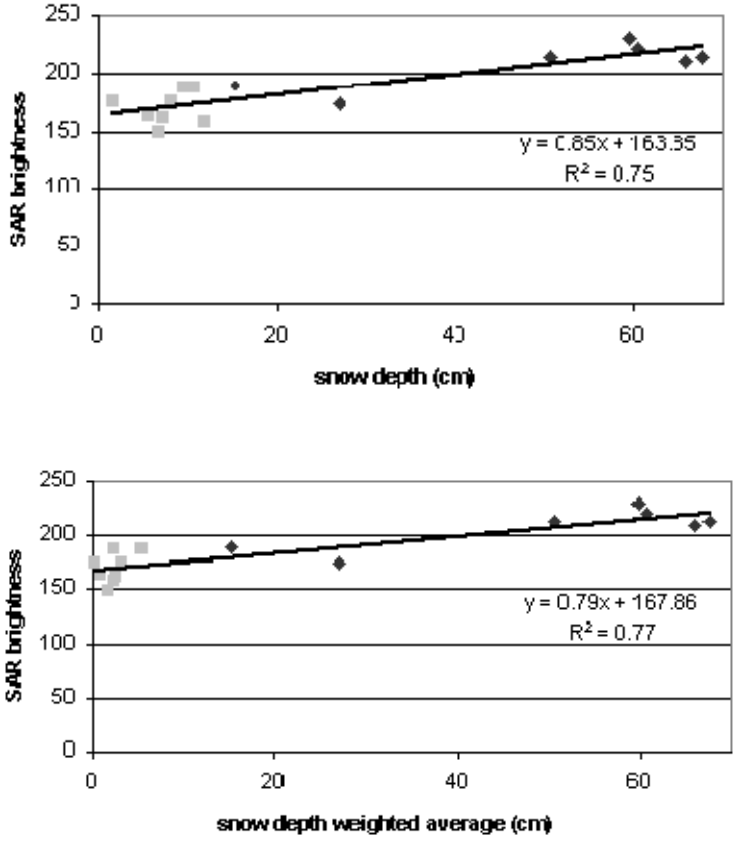

Figure 7.4 ERS-2 brightness to snow depth

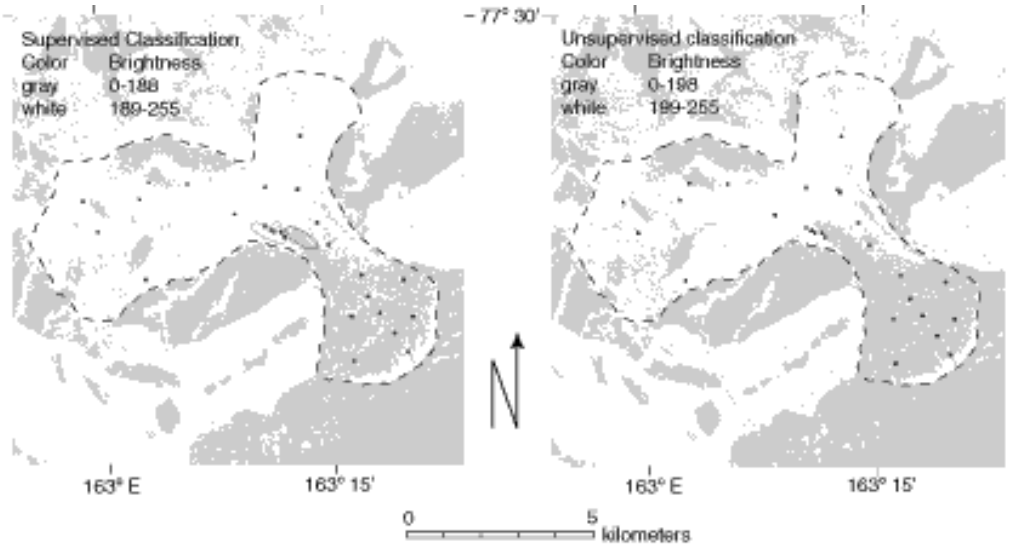

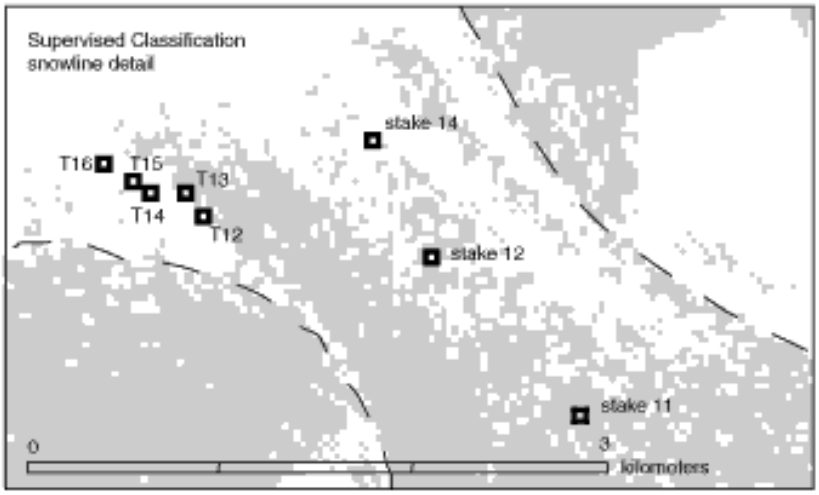

Figure 7.6: Commonwealth Glacier ERS-2 SAR 1/15/1999 snowline classification maps. Approximate outline of glacier shown in dashed line, within the glacier area, gray pixels are classified as ice and white pixels as snow. Ovals on supervised classification image are the training areas locations. Both images ©1999 European Space Agency.

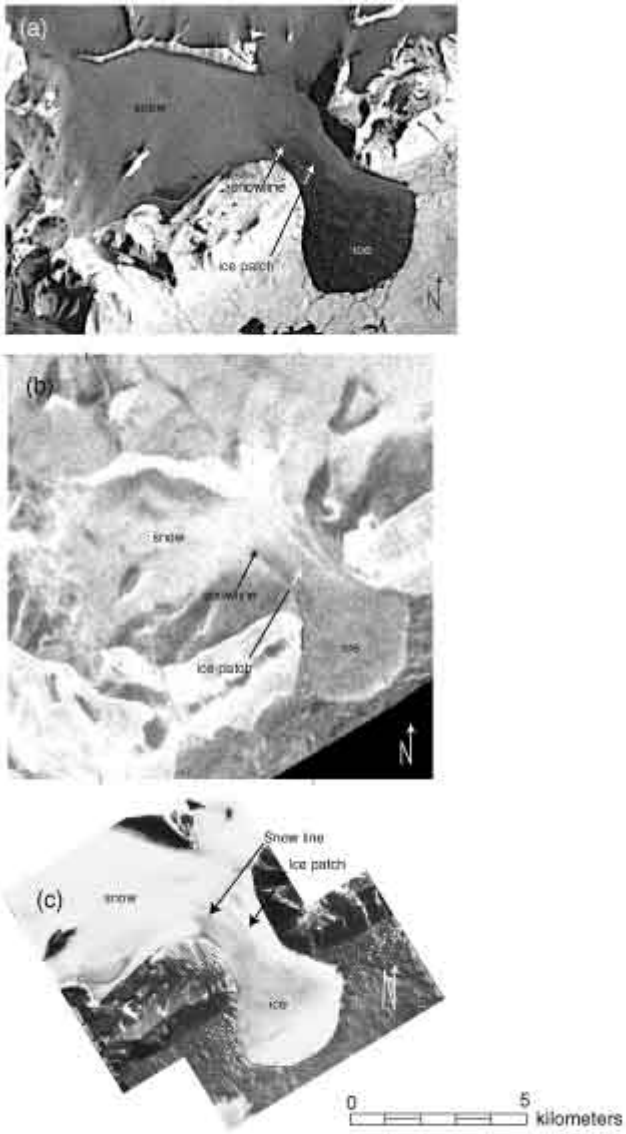

Figure 7.7: Comparison of Commonwealth Glacier. (a) January 6, 1993 Landsat 6 band 4 (J.C. Thomas, USGS). (b) ERS-2 January 15, 1999 ©1999 European Space Agency. (c) Two merged aerial photos taken November 1993 (USGS).

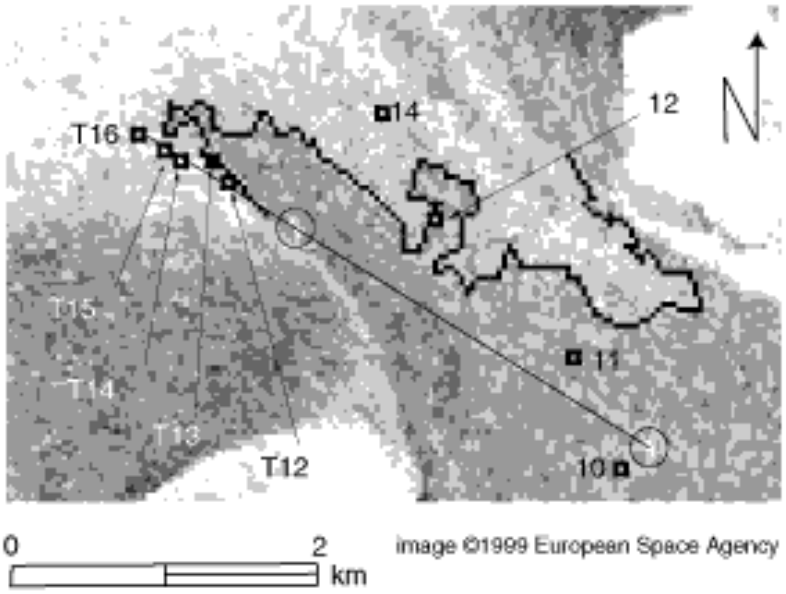

Figure 7.8: Detail of snowline on Commonwealth Glacier ERS-2 SAR 1/15/1999. Circles indicate reflectors, straight line is transect, and irregular line is SAR snowline.

113

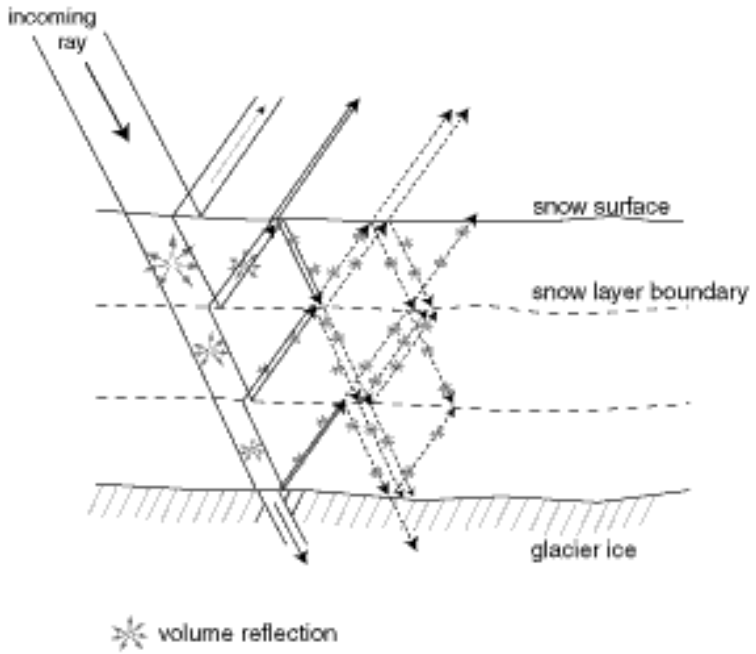

Figure 7.9: Enhanced volume backscatter.

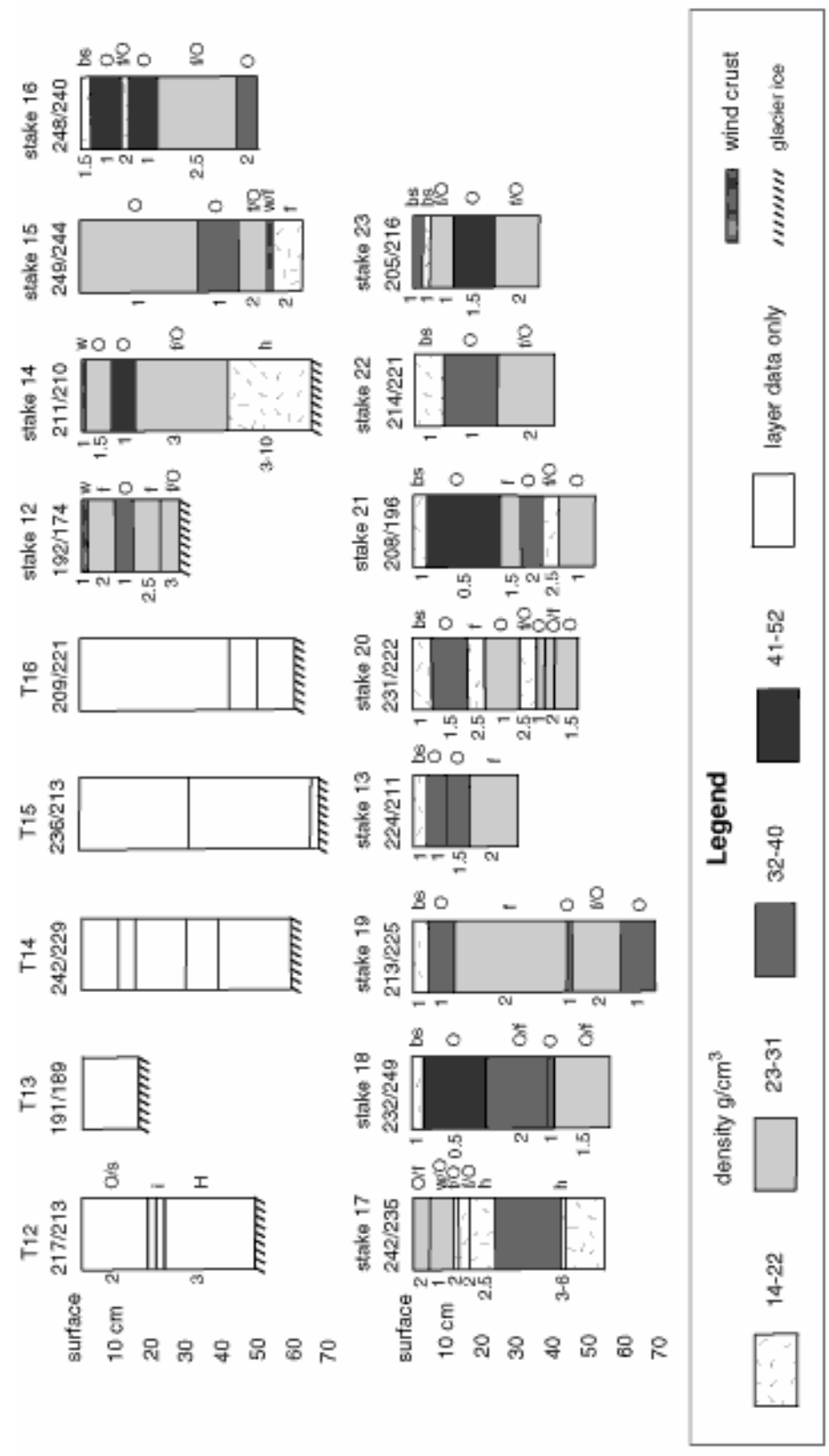

Figure 7.10: Commonwealth Glacier snow stratigraphy measured 1/19 to 1/20/99. Numbers to the far left indicate depth of layers. Grain size (mm) to the immediate left of layer. SAR brightness on top of each layer: first number is the exact location, the second number is a four-pixel average. T12, T13, T14, T15, T16, stake 12, and stake 14 show layers to glacier ice, all other locations to previous year snow surface. Mechanical structure to the right of layer: f—facets, O—rounds, w—wind crust, h—honeycomb, bs—broken stella, H—hoar, i—ice.

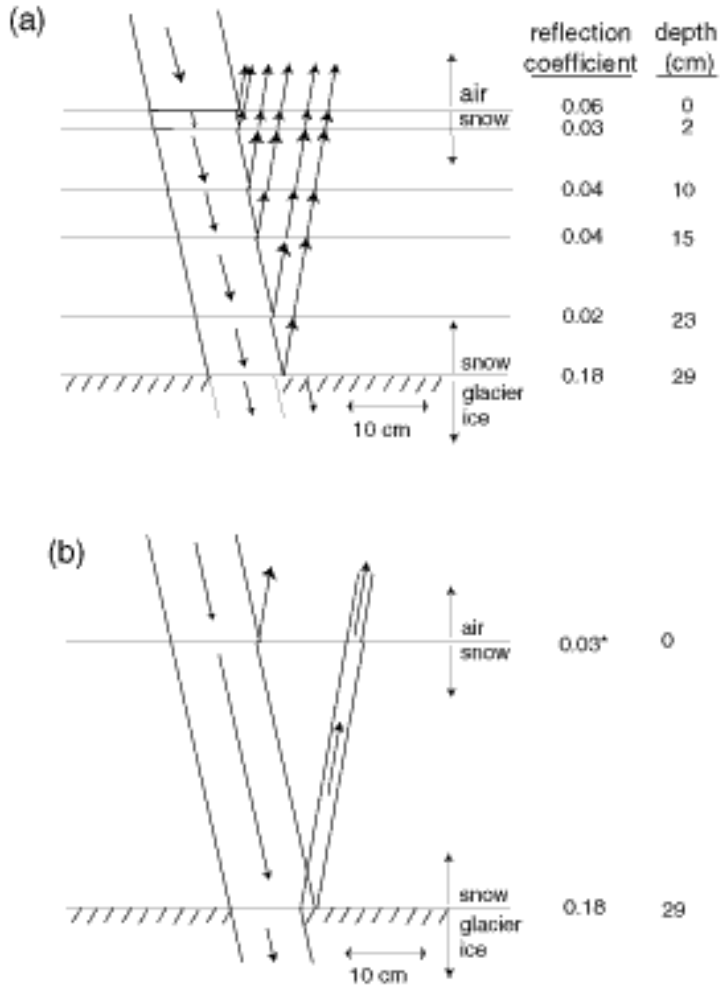

Figure 7.11: Reflections and refraction of the SAR beam at stake 12. Arrows indicate less than 10% of original power. (a) All layers recorded at stake 12. (b) Estimated refractions and reflections at stake 12 if there were no intervening layers.

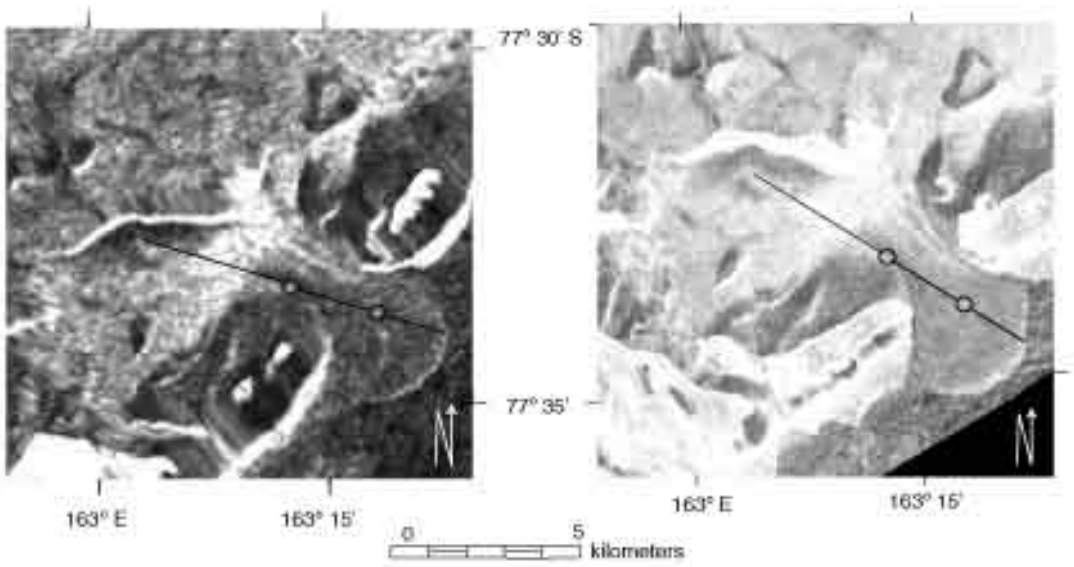

Figure 7.13: Terrain corrected SAR image transect locations. (a) 1/19/1999 Radarsat ScanSAR (image ©1999 Canadian Space Agency), (b) 1/15/1999 ERS-2 (image ©1999 European Space Agency). Reflector locations indicated by circles, transect indicated by line.

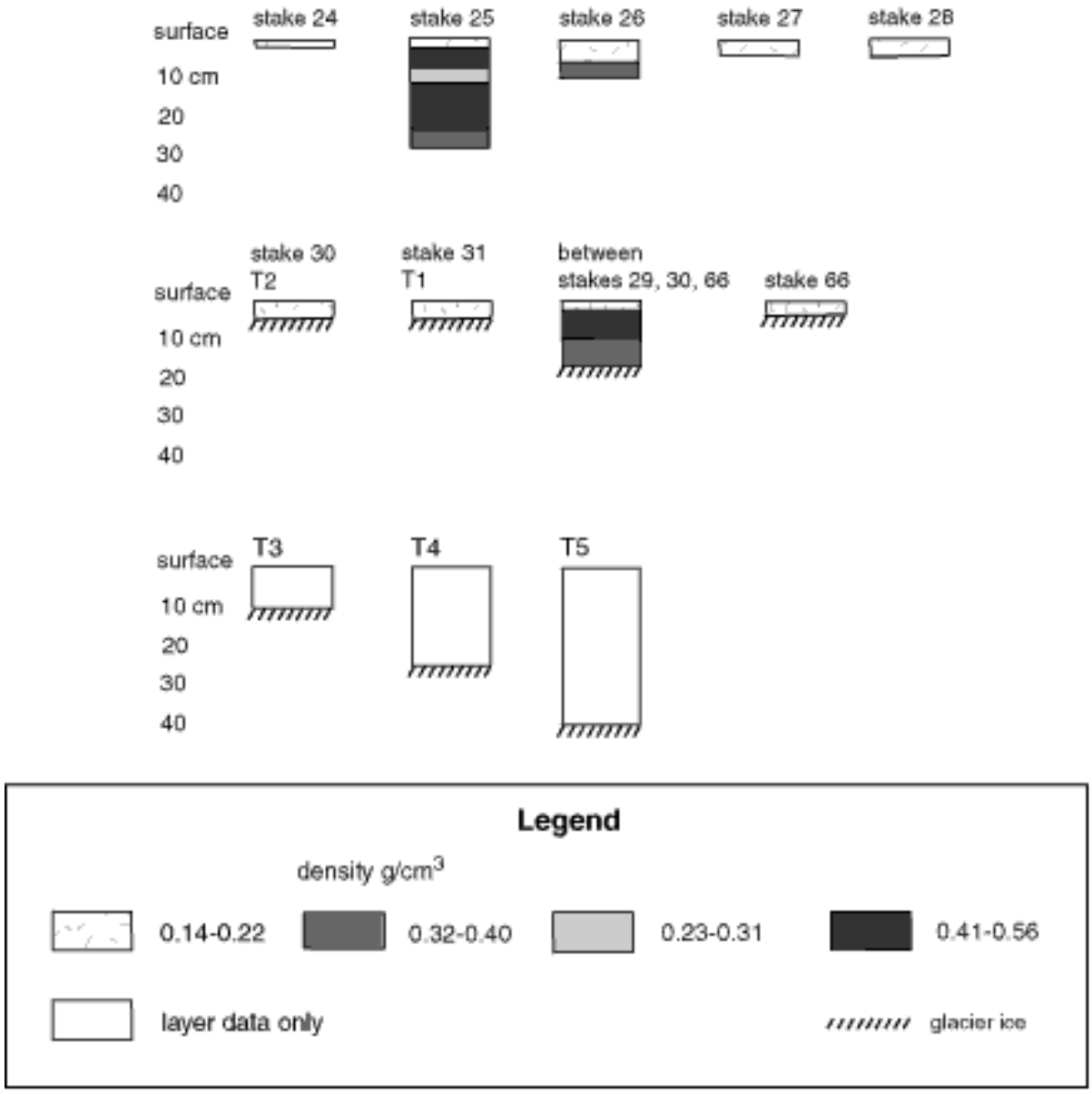

Figure 7.16: Howard Glacier snow layers graph. All measurements to previous year snow surface or glacier ice. Sites 30, 31, 66 are in ablation area. T3-T5 depths determined with probe rod and no layer data taken.

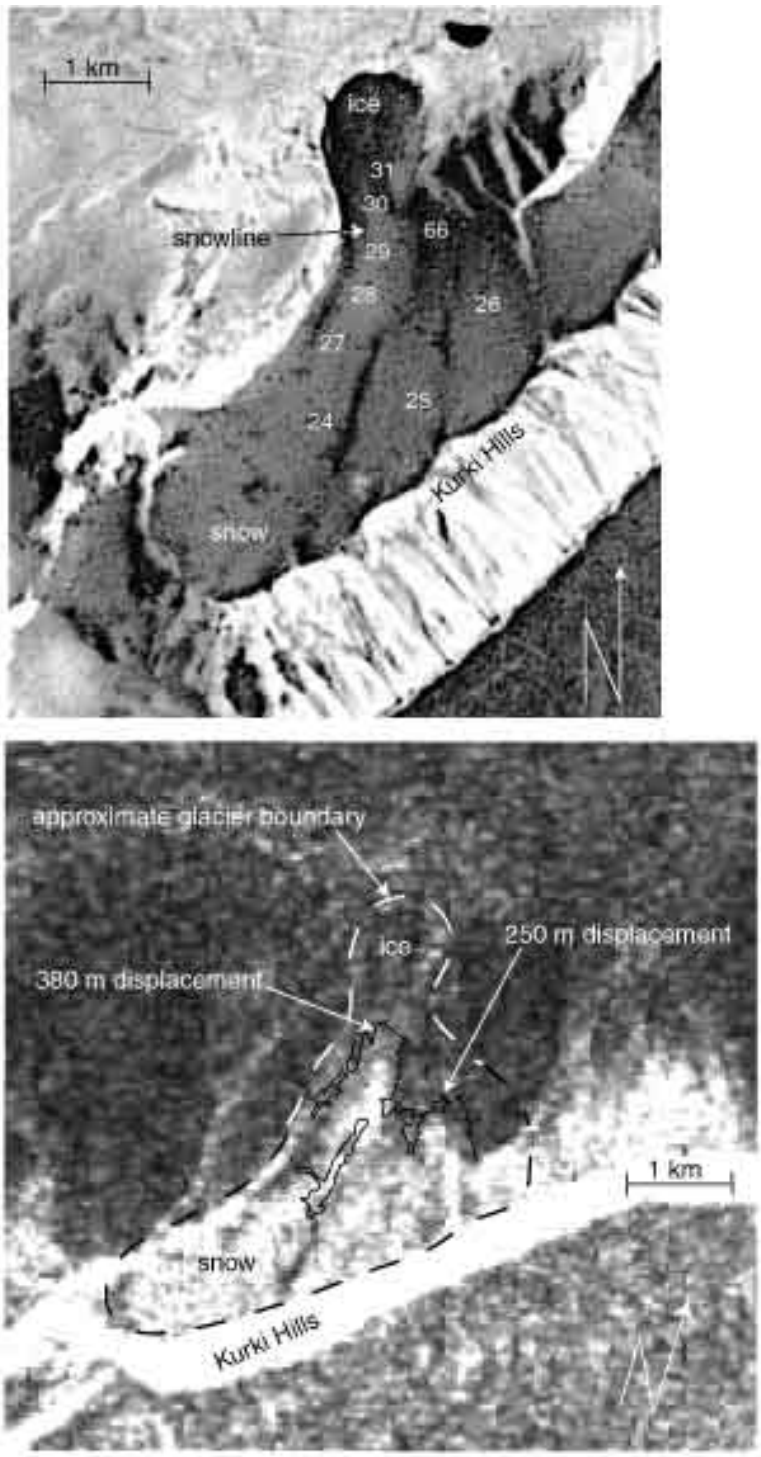

Figure 7.17: Landsat and Radarsat comparison of Howard Glacier snowline.
(a) January 6, 1993 Landsat 6 band 4 image, numbers indicate stake location
(b) January 19, 1999 Radarsat ScanSAR. The black line is the snowline from
(a) placed to a visual approximation of its proper location.

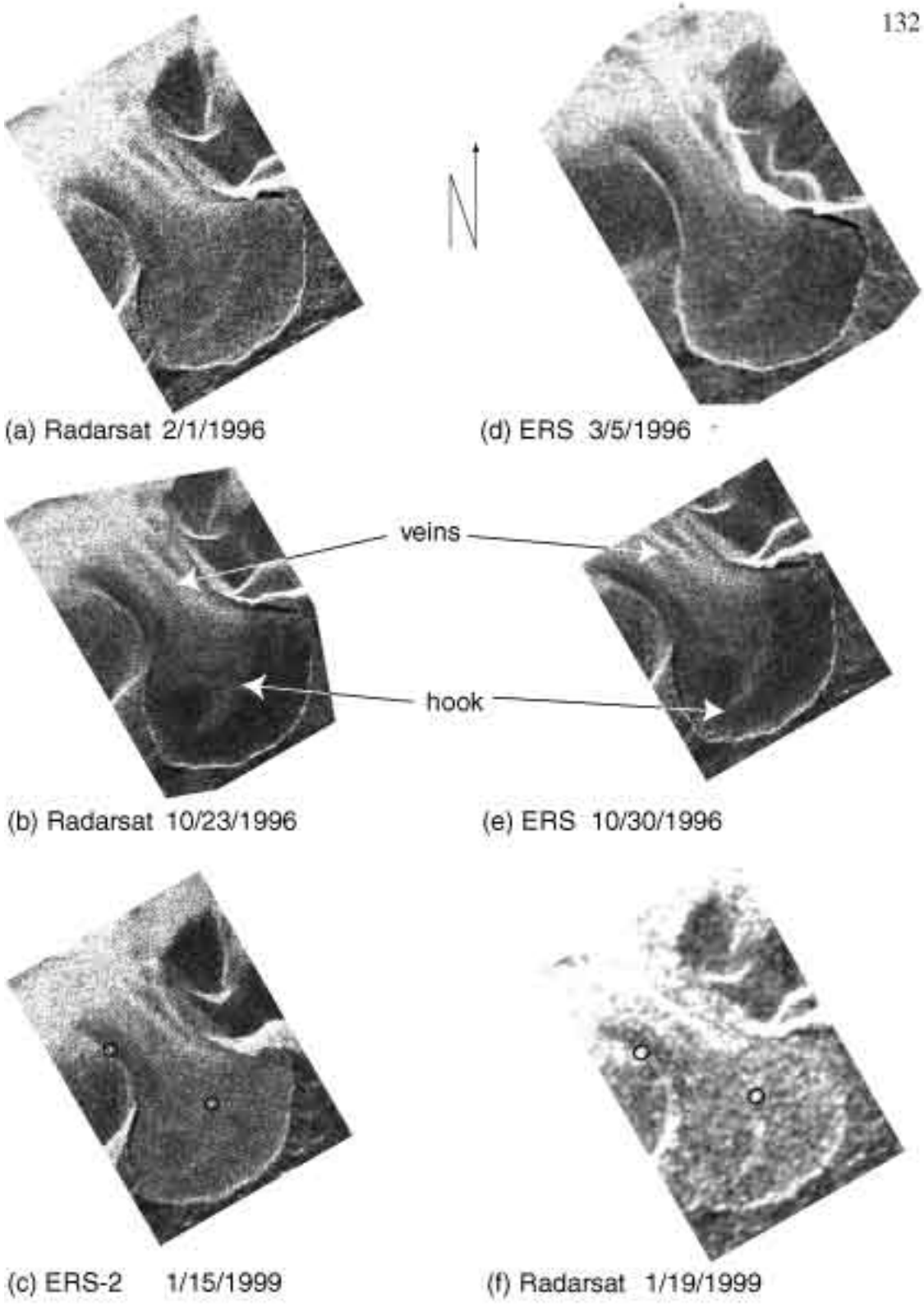

Figure 7.18: Six SAR views of Commonwealth Glacier. Reflectors highlighted with circles.

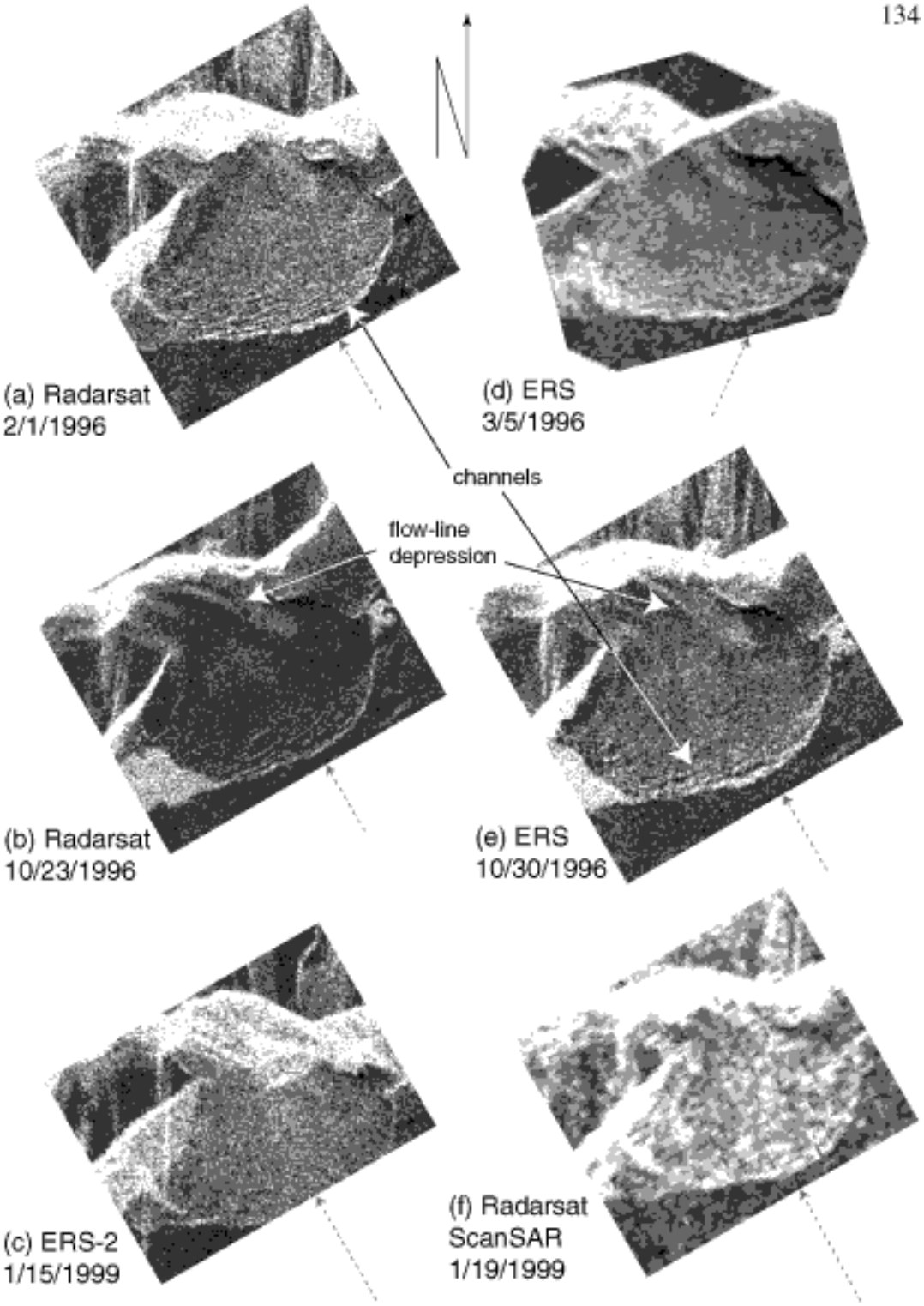

Figure 7.19: The terminus of Canada Glacier as represented by six uncorrected SAR images. Dashed arrow indicates SAR beam direction.

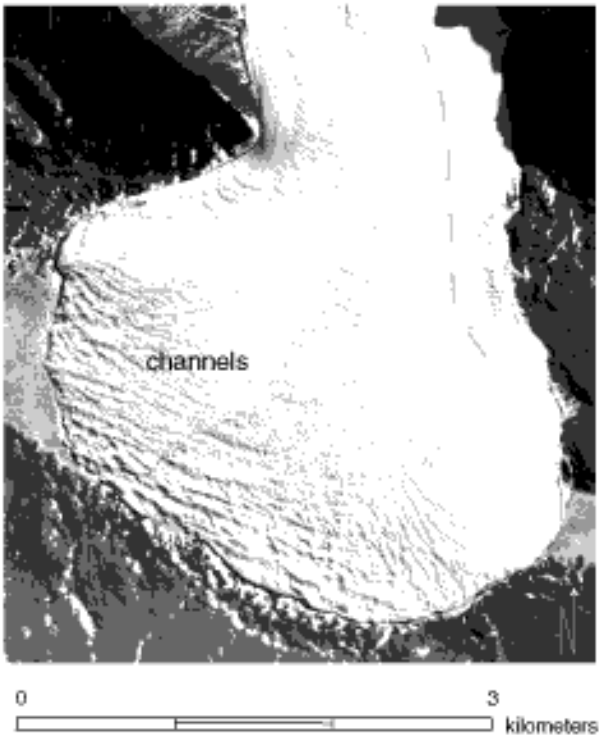

Figure 7.20: Aerial photo of Canada Glacier taken November 1993 (INSTARFF MCM LTER website). Dashed line shows approximate location of the flow linee depression.

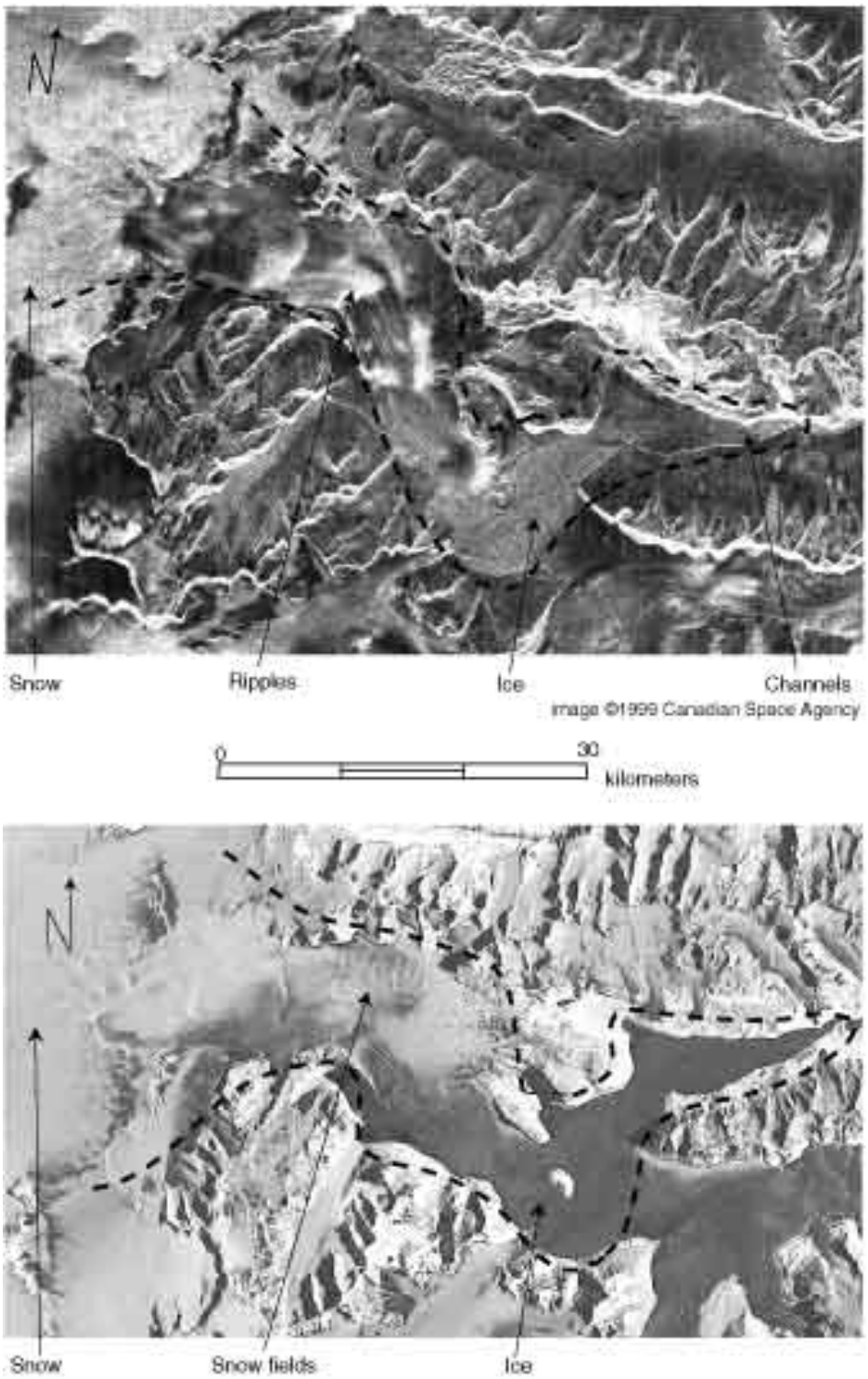

Figure 7.21: Images of Taylor Glacier. (a) January 19, 1999 Radarsat uncorrected ScanSAR. (b) January 6, 1993 Landsat 6 (band 4). Taylor Glacier indicated by dashed line.

Radarsat 2/1/1996

Radarsat ScanSAR 1/19/1999

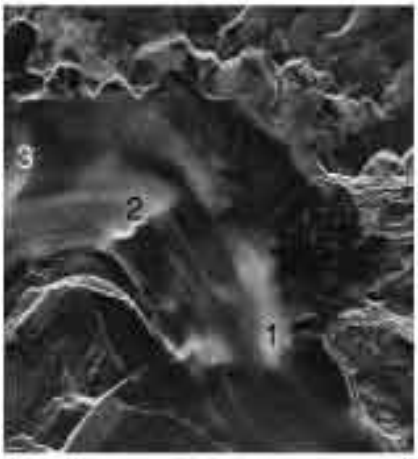

Radarsat 10/23/1996

ERS 10/30/1996

Landsat 6, band 4 3/16/1999

Figure 7.22: Ripples on the upper Taylor Glacier as represented by four SAR images and one Landsat. Numbers on images indicate ripple number. (ERS 3/5/1996 and 1/19/1999 did not image Taylor Glacier ripples.)

Radarsat 2/1/1996

ERS 3/5/1996

Radarsat 10/23/1996

ERS 10/30/1996

Radarsat 1/19/1999

Figure 7.23: Lower Taylor Glacier as nroresented by five SAR images.

142

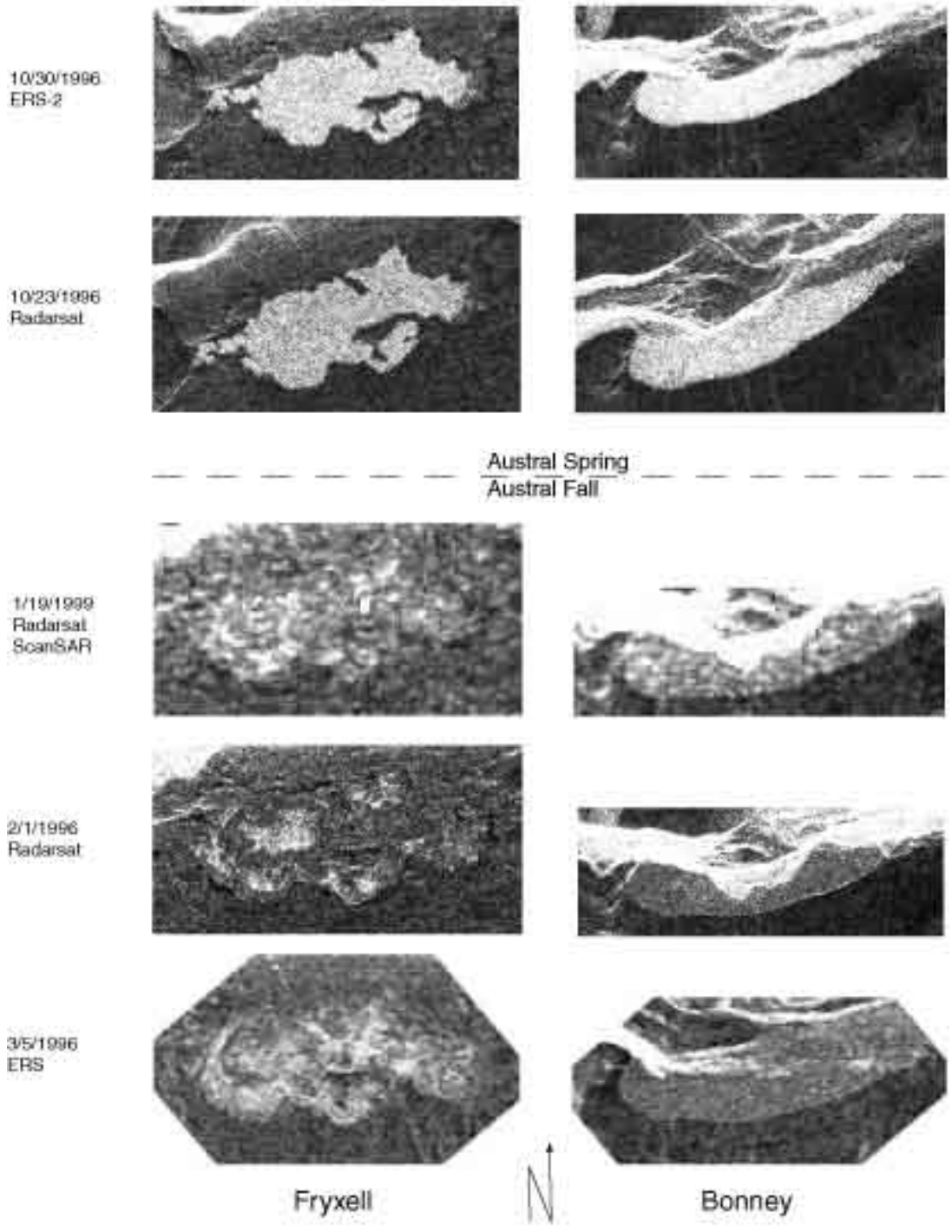

Figure 7.25: Comparison of backscatttt‹ of lake surfaces t t: season.

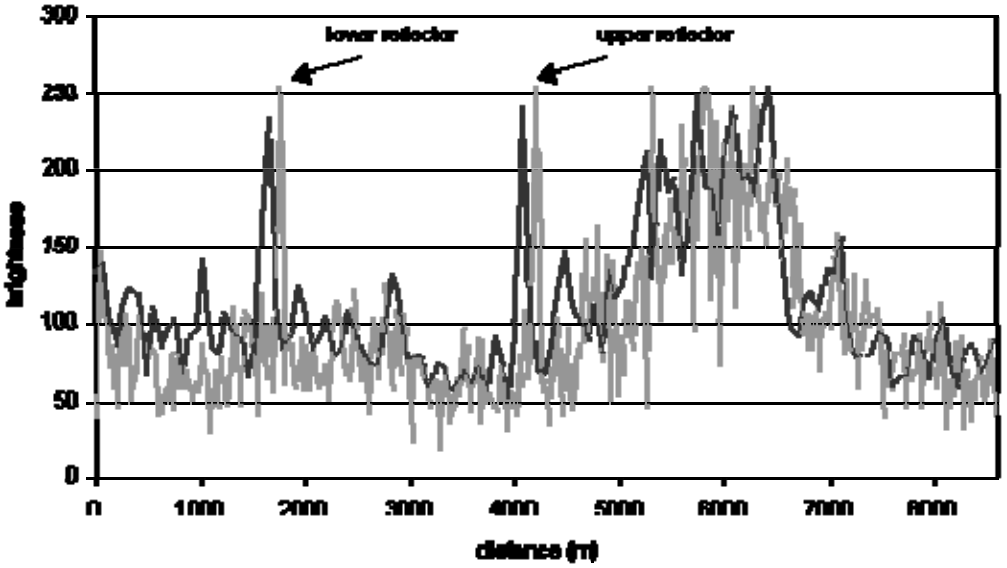
lower reflector
upper reflector
brightness
distance (m)
0
50
100
150
200
250
300
0
1000
2000
3000
4000
5000
6000
7000
8000

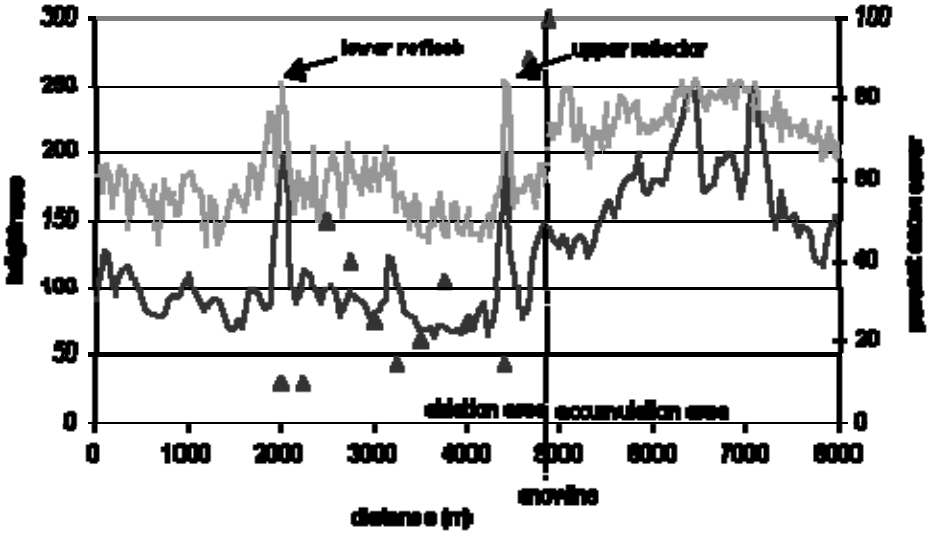
lower reflector
upper reflector
brightness
300
250
200
150
100
50
0
100
80
60
40
20
0
0
1000
2000
3000
4000
5000
6000
7000
8000
distance (m)

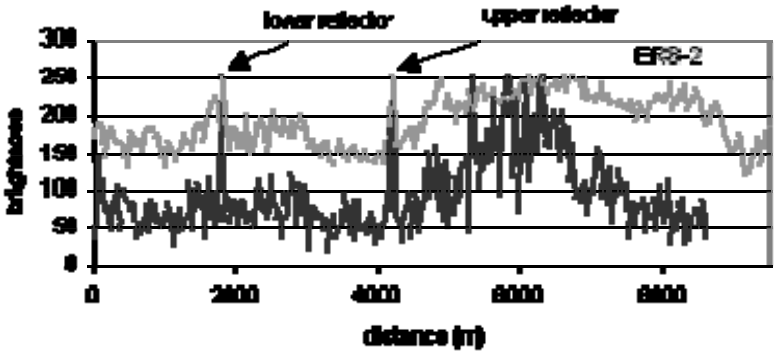
lower reflector
upper reflector
ERS-2
brightness
300
250
200
150
100
50
0
0
2000
4000
6000
8000
distance (m)

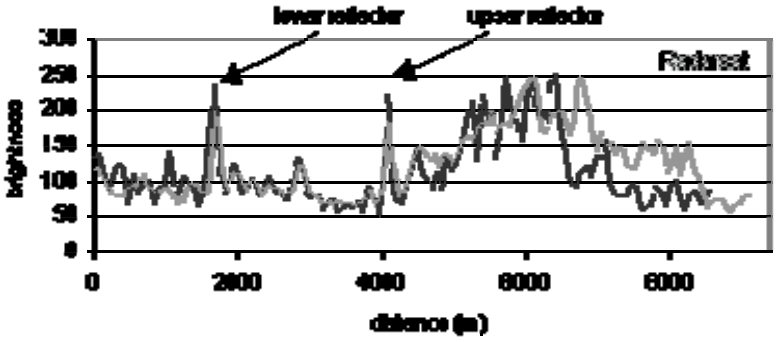
lower reflector
upper reflector
Radarsat
brightness
300
250
200
150
100
50
0
0
2000
4000
6000
8000
distance (m)

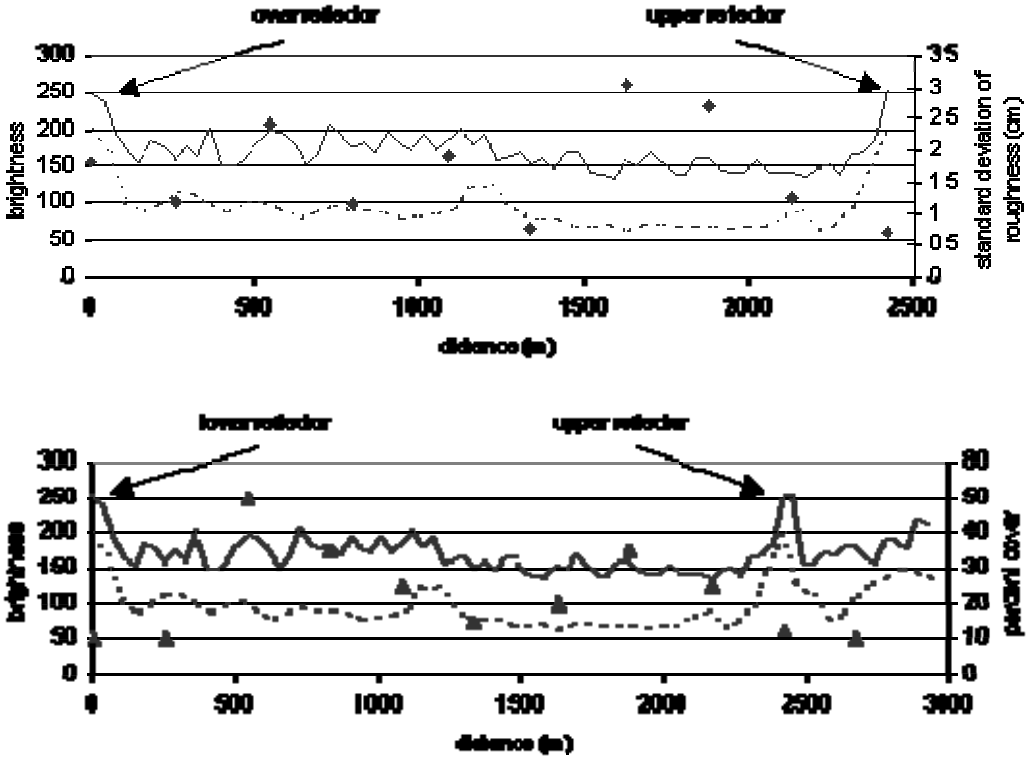
overwidow
upper window
brightness
standard deviation of roughness (cm)
distance (m)
lower window
upper window
brightness
percent cover
distance (m)

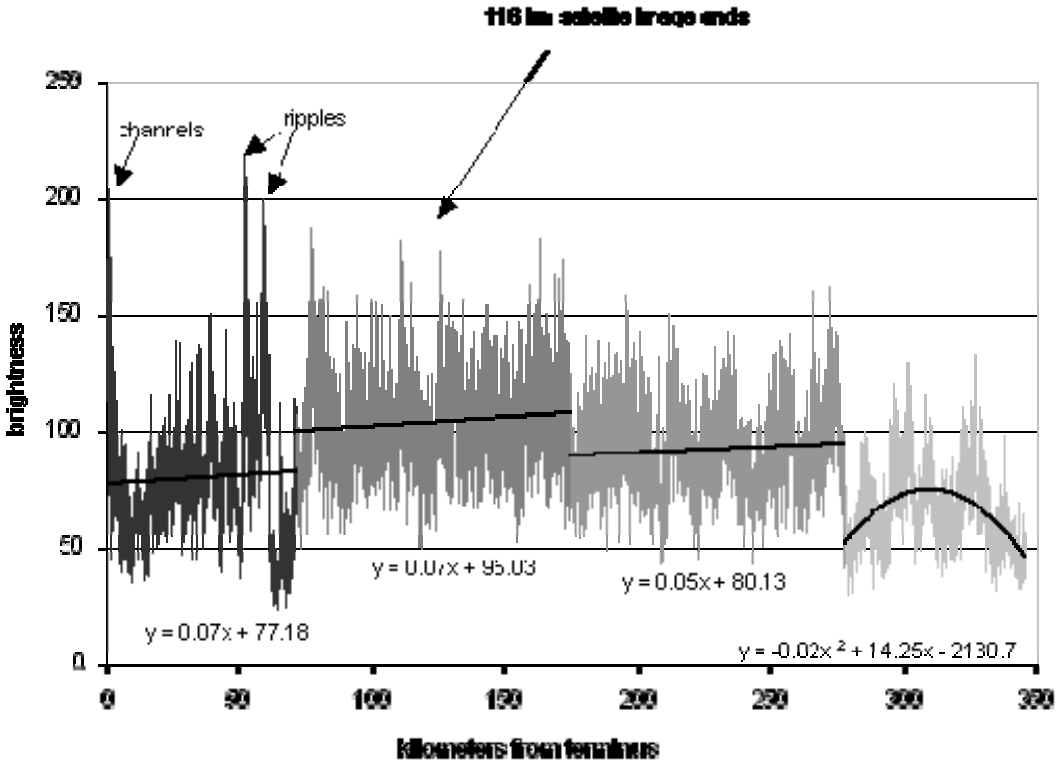
116 km satellite image ends
channels
ripples
brightness
y = 0.07x + 77.18
y = 0.05x + 80.13
y = -0.02x² + 14.25x - 2130.7
kilometers from terminus

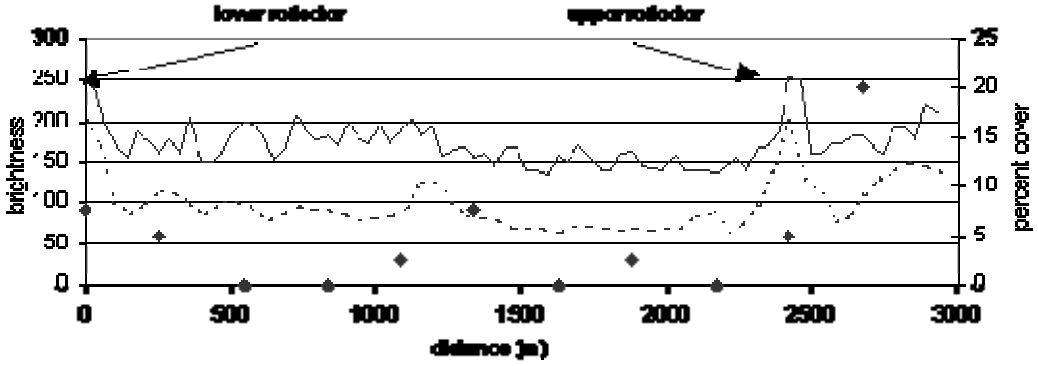
lower sollecker
upper sollecker
brightness
percent cover
distance (m)